



Integration of numerical modeling and Bayesian analysis for setting water quality criteria in Hamilton Harbour, Ontario, Canada

Maryam Ramin^a, Serguei Stremilov^a, Tanya Labencki^b, Alexey Gudimov^a, Duncan Boyd^b, George B. Arhonditsis^{a,*}

^a Ecological Modeling Laboratory, Department of Physical & Environmental Sciences, University of Toronto, Toronto, Ontario, Canada M1C 1A4

^b Water Monitoring & Reporting Section, Environmental Monitoring and Reporting Branch, Ontario Ministry of the Environment, Toronto, Ontario, Canada M9P 3V6

ARTICLE INFO

Article history:

Received 16 February 2010

Received in revised form

31 August 2010

Accepted 31 August 2010

Available online 4 December 2010

Keywords:

Phosphorus loading

Eutrophication modeling

Risk assessment

Hamilton Harbour

Ecosystem restoration

Top-down control

Benthic–pelagic coupling

ABSTRACT

The credibility of the scientific methodology of mathematical models and their adequacy to form the basis of public policy decisions has frequently been challenged. We believe that the development of novel methods for rigorously assessing model uncertainty should be a top priority of the modeling community. In this regard, we introduce the Bayesian calibration of process-based models as a methodological advancement that warrants consideration in aquatic ecosystem research. This modeling framework combines the advantageous features of both mechanistic and statistical approaches, i.e., mechanistic understanding that remains within the bounds of data-based parameter estimation. Other advantages of the Bayesian approach are the ability to sequentially update “beliefs” as new knowledge is available, the consistency with the scientific process of progressive learning and the policy practice of adaptive management. In this study, the Bayesian calibration framework is used to guide the water quality criteria setting process in Hamilton Harbour, Ontario, Canada. First, we present the results of the Bayesian calibration exercise and examine the ability of the model to adequately reproduce the average observed patterns along with the major cause–effect relationships underlying the Harbour water quality conditions. We then address the following critical questions regarding the future response of the system: How possible is it to meet the objective of delisting the study system as an Area of Concern, if the nutrient loading reductions proposed by the Hamilton Harbour Remedial Action Plan are actually implemented? What additional remedial actions are needed to increase the likelihood of meeting the water quality targets? In this regard, the present modeling study undertakes an estimation of the critical nutrient loads in the Harbour based on acceptable exceedance frequencies and confidence of compliance levels with different water quality criteria, e.g., chlorophyll *a*, total phosphorus (TP). Our analysis suggests that the water quality goals for TP ($17 \mu\text{g L}^{-1}$) and chlorophyll *a* concentrations ($5\text{--}10 \mu\text{g L}^{-1}$) will likely be met, if the recommendation for phosphorus loading at the level of 142 kg day^{-1} is achieved. We also provide evidence that the anticipated structural shifts of the zooplankton community will determine the restoration rate of the Harbour. Finally, we pinpoint two critical aspects of the system dynamics that invite further investigation and will likely modulate the stability of the new trophic state, i.e., the coupling between the benthic and pelagic habitat and the relative importance of the allochthonous organic matter in sustaining the secondary production in the system.

© 2010 Elsevier Ltd. All rights reserved.

1. Introduction

Water quality management relies upon the establishment of criteria used as measurable surrogates for the beneficial uses of waterbodies. Because violation of these criteria is typically the basis for regulatory enforcement and listing of the systems as Areas of

Concern (Borsuk et al., 2002), Reckhow et al. (2005) argued that the first critical decision in the criteria selection process is the identification of a measurable water quality characteristic that is a reliable predictor of the attainment of the beneficial (or designated) use. The next step usually involves the identification of the optimal numerical value of the water quality variable selected (i.e., the criterion level) that allows the discrimination between impaired and non-impaired conditions, while accounting for the inevitable tradeoffs between environmental protection and socioeconomic concerns (Barnett and O'Hagan, 1997). Beyond that, another key

* Corresponding author. Tel.: +1 416 208 4858; fax: +1 416 287 7279.

E-mail address: georgea@utsc.utoronto.ca (G.B. Arhonditsis).

feature of a water quality criterion is the selection of an adequate resolution in space (e.g., spatial averages throughout the system or water quality trends of an offshore site) and time (e.g., annual/summer averages or samples from individual samplings) that will objectively reflect the ecosystem state. In particular, if we opt for a finer spatiotemporal resolution, then the water quality criteria setting process should also accommodate the natural variability or the uncertainty in forecasting aquatic ecosystem dynamics by explicitly acknowledging that the expectation of 100% attainment of the criterion level at all locations in a waterbody and at all times is unrealistic (Borsuk et al., 2002; Reckhow et al., 2005; Zhang and Arhonditsis, 2008). Finally, once the water quality criterion is set, the evaluation of the current and future compliance of the waterbody requires an operational procedure that is usually founded upon the collection of a sufficient number of samples together with a statistical test and/or a process-based model that should effectively link management actions with the system response (Borsuk et al., 2002; Arhonditsis et al., 2007).

In the context of water quality assessment, the application of process-based (or mechanistic) models typically has a deterministic character in that single-value predictions at each point in time and space are derived from uniquely determined model inputs, while most of the existing calibration efforts aim at reproducing the average ecological dynamics but fail to capture the entire range of conditions experienced in the system (Pace, 2001). The credibility of this practice and its adequacy in addressing environmental management problems has recently been questioned for two main reasons (Clark et al., 2001; Borsuk et al., 2002; Arhonditsis and Brett, 2004; Stow et al., 2009). First, regardless of its complexity and supporting information, the application of any modeling construct involves substantial uncertainty contributed by model structure, parameters, and other associated inputs (inaccurate boundary or initial conditions). All models, by definition, are drastic simplifications of reality that merely approximate the actual processes, i.e., all parameters are essentially spatially and temporally averaged values unlikely to be represented by fixed constants, and therefore the strict determinism that disregards the uncertainty in aquatic ecosystem modeling misleadingly omits the risks associated with different remedial actions (Arhonditsis et al., 2006). Second, some models developed to depict the average ecosystem behavior are inadequate in addressing the type of percentile-based standards needed to accommodate the natural spatiotemporal variability and may bias (underestimate) the predictions of the frequency of standard violations under various management options (Borsuk et al., 2002). For better model-based decision analysis that can effectively support the development of environmental standards and the policy making process, the uncertainty in model predictions as well as the full range of the expected system responses must be rigorously quantified and reported in a straightforward way (Arhonditsis et al., 2007).

Hamilton Harbour, a large eutrophic embayment located at the western tip of Lake Ontario (Fig. 1), has water quality goals that encompass the complex interplay among abiotic and biotic components pertinent to its beneficial uses (Hiriart-Baer et al., 2009). Specifically, local stakeholders have selected the warm water fishery as a priority use for the Harbour which was then related to a critical total phosphorus (TP) level following a conceptual model that dissected the eutrophication problem in the Harbour into a sequence of causal associations, i.e., fish need aquatic plants for shelter and reproduction, aquatic plants need light to grow, light will only penetrate the water column if chlorophyll *a* levels are sufficiently low, low chlorophyll *a* levels are achieved through sufficiently low TP concentrations. The next step involved the selection of critical thresholds for the management-relevant water quality variables that aimed to effectively integrate

environmental concerns with local socioeconomic values (Hall et al., 2006). In particular, based on a framework that involved data analysis, expert judgment, and modeling, the TP concentration target was set at $17 \mu\text{g L}^{-1}$, while the environmental goals related to chlorophyll *a* concentrations ($5\text{--}10 \mu\text{g L}^{-1}$) and Secchi disc depth (3.0 m) emerged through a consensus on what were desirable and/or achievable targets for the Harbour (Charlton, 2001). Following this analytical approach, the maximum allowable exogenous TP loadings in the Harbour were set at 142 kg day^{-1} , based on predictions that these loads would achieve compliance with the water quality goals. However, the development of the stressor–effect relationships (exogenous nutrient loading–system responses) that provided the basis of the management actions in the Harbour has neither accommodated the uncertainty underlying model predictions along with natural ecosystem variability, nor has it considered the pragmatic need of adopting percentile-based standards (Zhang and Arhonditsis, 2008).

In this study, we present a modeling exercise that aims to revisit the robustness of the existing total maximum daily loading decisions and to guide a water quality criteria setting process that explicitly acknowledges the likelihood of standard violations in Hamilton Harbour. The basis of our work is a Bayesian calibration framework founded upon a statistical formulation that explicitly accommodates measurement error, parameter uncertainty, and model structure imperfection (Arhonditsis et al., 2007). This Bayesian approach has been shown to provide realistic uncertainty estimates of ecological predictions; to alleviate the problem of model identifiability; to sequentially update model parameterization; to effectively support probabilistic inference on significant cause–effect relationships pertaining to water quality management as well as to maximize the value of information gained from environmental monitoring programs; and to simultaneously calibrate biogeochemical models at multiple systems, thereby allowing the effective modeling of sites with limited information (Arhonditsis et al., 2007, 2008a,b; Zhang and Arhonditsis, 2008; 2009). Our intent here is the illustration of a Bayesian methodological framework suitable to the decision making process by estimating the critical nutrient loads that can potentially result in acceptable probabilities of compliance with different water quality criteria. The analysis begins with the presentation of the model calibration exercise and examines the ability of the model to adequately reproduce the average observed patterns along with the major cause–effect relationships underlying the Harbour water quality conditions. We then address several critical questions regarding the present status and the future response of the system, such as: Is it possible to meet the objective of delisting the study system as an Area of Concern, if the nutrient loading reductions proposed by the Hamilton Harbour Remedial Action Plan are actually implemented? How frequently would the existing water quality criteria be violated and how confident are we that the exceedance frequency of these standards will remain lower than the U.S. EPA endorsed 10% level (Office of Water, 1997)? What additional remedial actions are needed to increase the likelihood of meeting the water quality targets?

2. Methods

2.1. Model description

This section provides a description of the basic conceptual design of the model. The flow diagrams of the nitrogen and phosphorus cycles of the model are depicted in Figs. 2 and 3, the definitions of the model parameters are given in Table 1, while the mathematical equations can be found in the Electronic Supplementary Material.

2.1.1. Model spatial structure and forcing functions

We considered a two-compartment vertical segmentation representing the epilimnion and hypolimnion of the Harbour. The depths of the two boxes varied

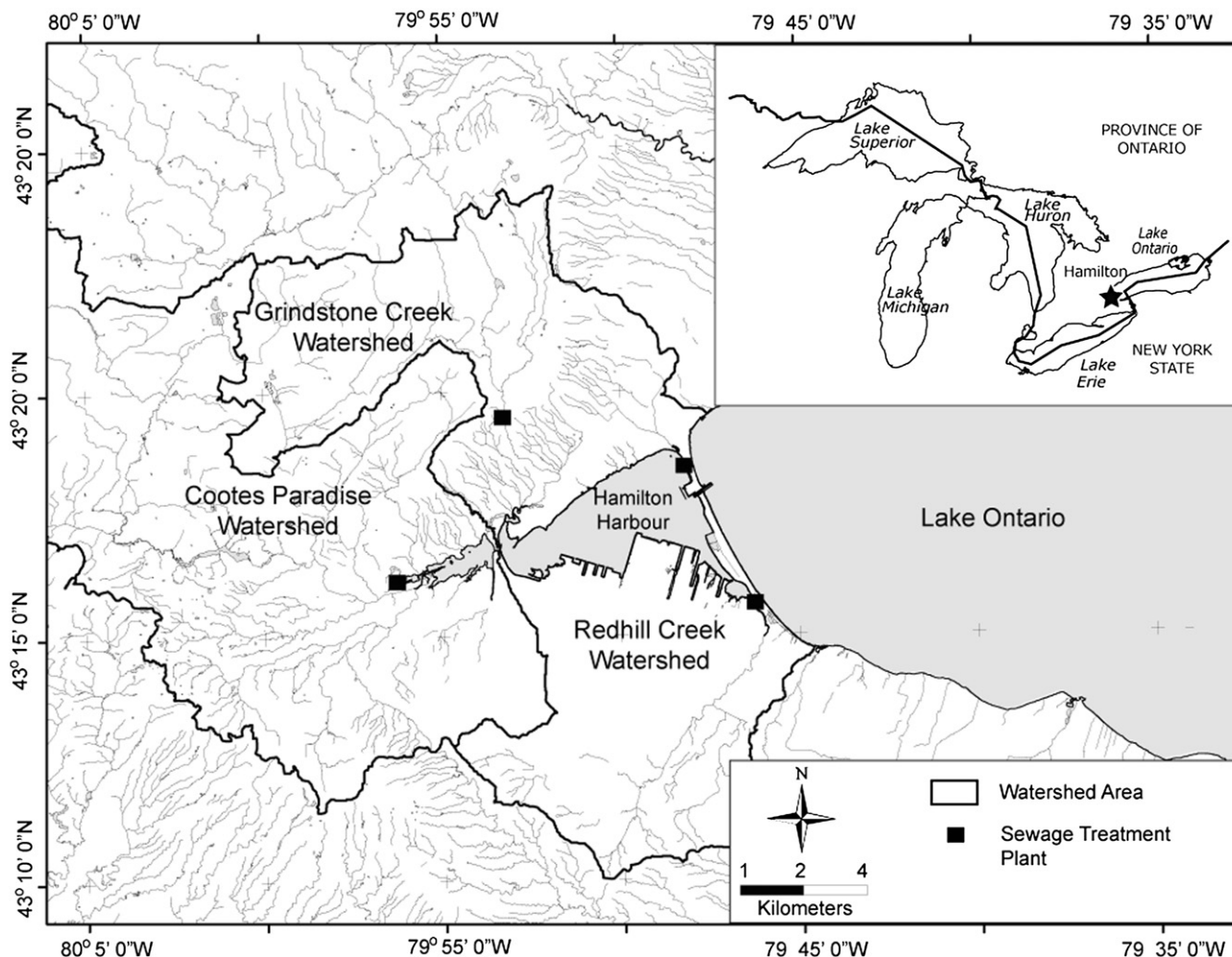


Fig. 1. Map of Hamilton Harbour, western end of Lake Ontario, and the major point and non-point loading sources in this system. The Red Hill Creek watershed includes the Woodward Avenue WWTW sewershed.

with time and were explicitly defined based on extensive field measurements for the study period 1987–2007 (Dermott et al., 2007; Hiriart-Baer et al., 2009). During the stratified period, the epilimnion was defined as the maximum depth where the water temperature varied ≤ 1 °C relative to the temperature at 0.5 m; otherwise, we assumed a box depth of 13 m and the mass exchanges between the two compartments were computed using Fick's Law (Klapwijk and Snodgrass, 1985; Hamblin and He, 2003). Other external forcing functions include the solar radiation, day length, precipitation, evaporation based on meteorological data from Environment Canada; namely, the Canadian Daily Climate Data (1996–2002) and the Canadian Climate Normals (1971–2000) (http://www.climate.weatheroffice.ec.gc.ca/prods_servs/index_e.html). Loads of inorganic nutrients and organic matter enter Hamilton Harbour from the following main sources: Red Hill and Grindstone creeks, combined sewer overflows (CSOs), ArcelorMittal Dofasco and U.S. Steel Canada steel mills, Woodward and Skyway wastewater treatment plants (WWTPs), and Cootes Paradise (Fig. 1). Estimates of flow and nutrient loadings are based on available data from the Water Survey of Canada (<http://www.wsc.ec.gc.ca/>) and the RAP loading report (Hamilton Harbour Technical Team: 1996–2002 Contaminant Loadings and Concentrations to Hamilton Harbour or HHTT-CLR, 2004). Similar to the practice presented by Arhonditsis and Brett (2005), the model was forced with the mean hydrological and nutrient loading seasonal cycle over the 1996–2002 period. Notably, to overcome the lack of data regarding the within-year variability of the external loading, it was assumed that the nutrient loading rates follow the precipitation month-to-month variability as calculated from the regional climate normal. Another critical assumption of our modeling exercise involves the dataset used to guide model calibration; in particular, we examined the capacity of the model to reproduce the post-2000 average observed patterns in the Harbour (Hiriart-Baer et al., 2009). The influence of the assumptions made regarding the nutrient loading estimates as well as the specification of the present water quality conditions in the Harbour on the projected trends will be further examined in subsequent work.

The exchanges between Hamilton Harbour and the relatively high quality waters of Lake Ontario through the Burlington Ship Canal are another major regulatory factor of the Harbour water quality associated with the dilution of the pollutant concentrations, the decrease of Harbour's residence time, and the oxygenation of the hypolimnetic waters (Barica, 1989; Hamblin and He, 2003). Winter exchanges are primarily driven by short-term oscillations due to water level differences at the two ends of the canal, while the exchanges during the summer stratified period are mediated by slowly fluctuating density gradients, i.e., warm Harbour water flowing into the lake from the top layer and colder lake water flowing into the Harbour in the bottom layer (see Figs. 1 and 2 in Barica, 1989). Existing evidence also suggests that the Hamilton Harbour-Lake Ontario interplay during the stratified conditions is much stronger and steadier than in winter (Hamblin and He, 2003). In this study, following the Klapwijk and Snodgrass (1985; see their Fig. 3) conceptual model, we assumed that 10% of the Lake Ontario inflows are directly discharged to the epilimnion, whereas 90% of the fresher oxygenated lake water replaces the hypolimnetic masses in the Harbour. The model considers an average hydraulic loading of $81.45 \times 10^6 \text{ m}^3$ from fluvial and aerial sources during the summer stratified period. The total (gross) inflows from Lake Ontario are $468 \times 10^9 \text{ m}^3$ corresponding to an average inflow rate of $45 \text{ m}^3 \text{ s}^{-1}$. After correcting for evaporative losses at the Harbour surface, these inputs represent an average residence time of 62 days during the stratified season, whereas the assumption that nearly all the Lake Ontario water enters the hypolimnion of the Harbour results in a hypolimnetic residence time of 31 days; both values are very close to those calculated by Hamblin and He (2003).

2.1.2. Equations

We developed an ecological model that considers the interactions among the eight state variables: nitrate (NO_3), ammonium (NH_4), phosphate (PO_4), (non-cyanobacteria) phytoplankton, cyanobacteria, zooplankton, organic nitrogen (ON) and organic phosphorus (OP).

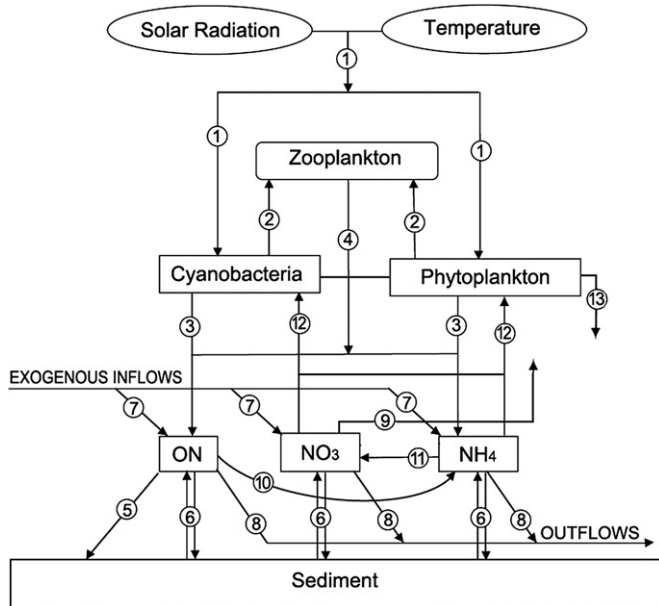


Fig. 2. The nitrogen biogeochemical cycle of the model: (1) external forcing for phytoplankton growth (temperature, solar radiation); (2) zooplankton grazing; (3) phytoplankton basal metabolism excreted as NH_4 and ON ; (4) zooplankton basal metabolism excreted as NH_4 and ON ; (5) settling of particles; (6) water sediment NO_3 , NH_4 , and ON exchanges; (7) exogenous inflows of NO_3 , NH_4 , and ON ; (8) outflows of NO_3 , NH_4 , and ON ; (9) NO_3 sinks due to denitrification; (10) ON mineralization; (11) nitrification; (12) phytoplankton uptake; and (13) phytoplankton settling.

2.1.3. Phytoplankton

The ecological submodel simulates two phytoplankton functional groups, labelled as “cyanobacteria” and “phytoplankton”, that differ with regards to their strategies for resource competition (nitrogen, phosphorus, light, and temperature) and metabolic rates as well as their settling velocities. The cyanobacteria-like group is modeled as K-strategist with low maximum growth and metabolic rates, slower P and faster N kinetics, low settling velocities, and high temperature optima. By contrast, the more generic “phytoplankton” group has attributes of r-selected

organisms with high maximum growth rates and higher metabolic losses, relatively fast phosphorus and slow nitrogen kinetics, low temperature optima, high sinking velocities and is considered to represent the average characteristics of the remaining phytoplankton community.

The governing equation for phytoplankton biomass accounts for phytoplankton production and losses due to mortality, settling, dreissenid filtration, and herbivorous zooplankton grazing. The phytoplankton growth is adjusted for water temperature conditions, nutrient and light availability. Phytoplankton growth temperature dependence has an optimum level (T_{opt}) and is modeled by a function similar to the Gaussian probability curve (Cercio and Cole, 1994; Arhonditsis and Brett, 2005). Phosphorus dynamics within the phytoplankton cells account for luxury uptake, i.e., phytoplankton nutrient uptake depends on both internal and external concentrations and is confined by upper and lower internal storage capacity (Hamilton and Schladow, 1997; Arhonditsis et al., 2002). Our model explicitly considers the role of new and regenerated production using separate formulations that relate phytoplankton uptake to the ambient nitrate and ammonium concentrations (Eppley–Peterson f -ratio paradigm; Eppley and Peterson, 1979). Regarding the dependence of photosynthesis on solar radiation, we used Steele’s equation coupled with Beer’s law to scale photosynthetically active radiation to depth. The extinction coefficient is determined as the sum of an assigned background light attenuation and attenuation due to chlorophyll a (Jassby and Platt, 1976). The phytoplankton mortality includes all internal processes that decrease algal biomass (respiration, excretion) as well as natural mortality and is assumed to increase exponentially with temperature. Phytoplankton settling considers the net change in biomass due to settling between adjacent compartments. We also incorporated a first-order loss rate representing the filtration from the zebra (*Dreissena polymorpha*) and quagga (*Dreissena bugensis*) mussels, which is a potentially important factor for phytoplankton biomass loss; especially in nearshore areas (Bastviken et al., 1998; Bierman et al., 2005).

2.1.4. Zooplankton

Zooplankton grazing and losses due to natural mortality/consumption by higher predators is the main two terms in the zooplankton biomass equation. Zooplankton has three food sources (the two phytoplankton groups and biogenic particulate matter or detritus) grazed with preference that changes dynamically as a function of their relative abundance (Fasham et al., 1990) [It should also be noted that the present model parameterization postulates a selective zooplankton preference for phytoplankton and detritus over cyanobacteria]. Zooplankton grazing was modeled using a Michaelis–Menten equation and the assimilated fraction of the grazed material fuels growth. In the absence of information to support more complex forms, we selected a linear closure term that represents the effects of a seasonally invariant predator biomass (see Edwards and Yool, 2000).

2.1.5. Nitrogen cycle

There are three nitrogen forms considered in the model: nitrate (NO_3), ammonium (NH_4), and organic nitrogen (ON) (Fig. 2). The ammonium equation considers the phytoplankton uptake and the proportion of phytoplankton and zooplankton mortality that is returned back to the water as ammonium. Ammonium is also oxidized to nitrate through nitrification and the kinetics of this process are modeled as a function of the ammonium, and the externally-forced dissolved oxygen, temperature, and light availability (Cercio and Cole, 1994; Tian et al., 2001). We used Wroblewski’s model (1977) to describe ammonium inhibition of nitrate uptake. The nitrate equation also takes into account ammonium oxidized to nitrate through nitrification and nitrate lost as nitrogen gas through denitrification. The latter process is modeled as a function of dissolved oxygen, temperature and the nitrate concentrations (Arhonditsis and Brett, 2005). The organic nitrogen equation considers the contribution of phytoplankton and zooplankton mortality to the organic nitrogen pool and the temperature-dependent mineralization that transforms organic nitrogen to ammonium. External nitrogen loads to the system and losses via the exchanges with Lake Ontario are also included.

2.1.6. Phosphorus cycle

Two state variables of the phosphorus cycle are considered in the model: phosphate (PO_4) and organic phosphorus (OP) (Fig. 3). The phosphate equation considers the phytoplankton uptake, the proportion of phytoplankton and zooplankton mortality/higher predation that is directly supplied into the system in inorganic form, the bacteria-mediated mineralization of organic phosphorus, and the net diffusive fluxes between adjacent compartments. We also accounted for phosphorus precipitation and subsequent sedimentation due to the iron loadings from two steel mills, based on an empirical equation originally implemented to correct for the observed Hamilton Harbour phosphorus concentrations (Hamilton Harbour Technical Team–Water Quality or HHTT-WQ, 2007). The effects of the uncertainty associated with this empirical relationship on the predicted outcomes will be considered in our analysis. The organic phosphorus equation also considers the amount of organic phosphorus that is redistributed through phytoplankton and zooplankton basal metabolism. A fraction of organic phosphorus settles to the sediment and another fraction is mineralized to phosphate through a first-order reaction. We also consider external phosphorus loads to the system and losses via the exchanges with Lake Ontario.

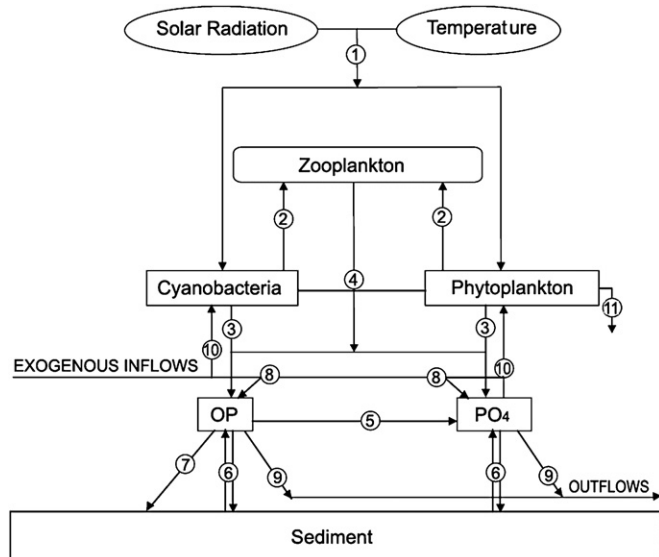


Fig. 3. The phosphorus biogeochemical cycle of the model: (1) external forcing to phytoplankton growth (temperature, solar radiation); (2) zooplankton grazing; (3) phytoplankton basal metabolism excreted as PO_4 and OP ; (4) zooplankton basal metabolism excreted as PO_4 and OP ; (5) OP mineralization; (6) water sediment PO_4 and OP exchanges; (7) settling of particles; (8) exogenous inflows of PO_4 and OP ; (9) outflows of PO_4 and OP ; (10) phytoplankton uptake; and (11) phytoplankton settling.

Table 1
Sensitivity of the posterior parameter distributions on the prior specifications.

Parameters	Description	Units	Priors		Posteriors			
			Min	Max	Loguniform		Lognormal	
					Mean	SD	Mean	SD
AH _(cy)	Half saturation constant for ammonium uptake by cyanobacteria	μg N L ⁻¹	30	80	58.72	14.18	55.67	10.56
AH _(phyt)	Half saturation constant for ammonium uptake by phytoplankton	μg N L ⁻¹	80	150	146.1	3.595	154.4	10.21
Denitrifmax	Maximum denitrification rate	μg N L ⁻¹ day ⁻¹	1	10	2.459	1.637	2.811	1.194
filter _(cy)	Filtering rate of cyanobacteria by dreissenids	day ⁻¹	0.0045	0.0245	0.0066	0.0015	0.0065	0.0013
filter _(phyt)	Filtering rate of phytoplankton by dreissenids	day ⁻¹	0.010	0.050	0.0106	0.0063	0.0080	0.0015
growthmax _(cy)	Cyanobacteria maximum growth rate	day ⁻¹	1.0	1.8	1.315	0.157	1.245	0.081
growthmax _(phyt)	Phytoplankton maximum growth rate	day ⁻¹	2.2	3.0	2.571	0.163	2.714	0.126
lk _(cy)	Half saturation light intensity for cyanobacteria	MJ/m ² day ⁻¹	100	250	202.8	30.13	182.6	19.82
lk _(phyt)	Half saturation light intensity for phytoplankton	MJ/m ² day ⁻¹	100	250	145.2	16.67	160.6	12.71
kbackground	Background light extinction coefficient	m ⁻¹	0.15	0.30	0.2646	0.0265	0.2392	0.0225
kchl a _(cy)	Self-shading effect for cyanobacteria	L (μg chl a m) ⁻¹	0.01	0.08	0.0338	0.0164	0.0289	0.0098
kchl a _(phyt)	Self-shading effect for phytoplankton	L (μg chl a m) ⁻¹	0.01	0.06	0.0579	0.0019	0.0633	0.0041
KCrefmineral	Organic carbon mineralization rate	day ⁻¹	0.0043	0.0243	0.0060	0.0010	0.0068	0.0016
KNrefmineral	Nitrogen mineralization rate	day ⁻¹	0.0043	0.0243	0.0065	0.0013	0.0083	0.0018
KPrefmineral	Phosphorus mineralization rate	day ⁻¹	0.0043	0.0243	0.0128	0.0014	0.0099	0.0015
KZ	Half saturation constant for zooplankton grazing	μg C/L	80	120	107.5	6.098	102.8	5.436
max grazing	Zooplankton maximum grazing rate	day ⁻¹	0.40	0.60	0.465	0.011	0.470	0.009
mp _(cy)	Cyanobacteria mortality rate	day ⁻¹	0.01	0.05	0.013	0.002	0.015	0.001
mp _(phyt)	Phytoplankton mortality rate	day ⁻¹	0.01	0.05	0.015	0.003	0.021	0.003
mz	Zooplankton mortality rate	day ⁻¹	0.14	0.19	0.158	0.004	0.160	0.004
NH _(cy)	Half saturation constant for nitrate uptake by cyanobacteria	μg N/L	30	80	52.37	14.58	49.48	9.356
NH _(phyt)	Half saturation constant for nitrate uptake by phytoplankton	μg N/L	80	150	112.4	19.79	110.9	13.41
Nitrifmax	Maximum nitrification rate	μg N/L ⁻¹ day ⁻¹	10	30	12.14	1.557	13.82	1.528
PH _(cy)	Half saturation constant for phosphorus uptake by cyanobacteria	μg P/L	18	30	24.85	3.632	23.09	1.998
PH _(phyt)	Half saturation constant for phosphorus uptake by phytoplankton	μg P/L	5	15	10.55	3.016	10.22	1.732
Pmaxuptake _(cy)	Maximum phosphorus uptake rate for cyanobacteria	μg P/L ⁻¹ day ⁻¹	0.005	0.025	0.010	0.002	0.010	0.001
Pmaxuptake _(phyt)	Maximum phytoplankton uptake rate for phytoplankton	μg P/L ⁻¹ day ⁻¹	0.01	0.05	0.021	0.004	0.021	0.003
Vsettling	Autochthonous particle settling velocity	m day ⁻¹	0.50	1.50	0.627	0.013	0.645	0.014
Vsettling _(biogenic)	Biogenic particle settling velocity	m day ⁻¹	0.35	1.75	0.481	0.110	0.591	0.140
Vsettling _(cy)	Cyanobacteria settling velocity	m day ⁻¹	0.01	0.05	0.036	0.007	0.030	0.007
Vsettling _(phyt)	Phytoplankton settling velocity	m day ⁻¹	0.12	0.25	0.212	0.108	0.199	0.164
β _N	Fraction of refractory nitrogen buried into deeper sediment		0.30	0.60	0.36	0.036	0.37	0.038
β _P	Fraction of refractory phosphorus buried into deeper sediment		0.80	0.95	0.93	0.011	0.92	0.013

2.1.7. Fluxes from the sediment

As a first approximation to model the role of the sediments, we followed a simple dynamic approach that relates the fluxes of nitrogen and phosphorus from the sediment with the algal and particulate matter sedimentation and burial rates, while also accounting for the role of temperature and dissolved oxygen (Arhonditsis and Brett, 2005). The relative magnitudes of ammonium and nitrate fluxes were also determined by nitrification and denitrification occurring at the sediment surface.

2.2. Bayesian framework

2.2.1. Statistical formulation

Our presentation examines a statistical formulation founded upon the assumption that the eutrophication model is an imperfect simulator of the environmental system but the model error is invariant with the input conditions, i.e., the difference between model and system dynamics was assumed to be constant over the annual cycle for each state variable. Our aim was to combine field observations with simulation model outputs to update the uncertainty of model parameters, and then use the calibrated model to give predictions (along with uncertainty bounds) of the natural system dynamics. An observation i for the state variable j , y_{ij} , can be described as:

$$y_{ij} = f(\theta, x_i, y_0) + \delta_j \quad i = 1, 2, 3, \dots, n \text{ and } j = 1, \dots, m \quad (1)$$

where $f(\theta, x_i, y_0)$ denotes the eutrophication model, x_i is a vector of time dependent control variables (e.g., boundary conditions, forcing functions) describing the environmental conditions, the vector θ is a time-independent set of the calibration model parameters, y_0 corresponds to the vector of the concentrations of the sixteen state variables at the initial time t_0 (initial conditions), and δ_j is the stochastic term that accounts for the discrepancy between the model and the natural system. Under the normality and conditional independence assumptions, the likelihood function will be:

$$p(y|f(\theta, x, y_0)) = \prod_{j=1}^m (2\pi)^{-n/2} \left| \sum \delta_j \right|^{-1/2} \exp \left[-\frac{1}{2} [y_j - f_j(\theta, x, y_0)]^T \sum \delta_j^{-1} [y_j - f_j(\theta, x, y_0)] \right] \quad (2)$$

where m corresponds to the number of state variables of our model for which data are available ($m = 16$); n is the number of observations in time used to calibrate the model ($n = 12$ average monthly values); $y_j = [y_{1j}, \dots, y_{mj}]^T$ and $f_j(\theta, x, y_0) = [f_{1j}(\theta, x, y_0), \dots, f_{mj}(\theta, x, y_0)]^T$ correspond to the vectors of the field observations and model predictions for the state variable j ; $\Sigma \delta_j = I_n \times \sigma_j^2$ denotes the model structural error; I_n denotes the identity or unit matrix of size n ; and σ_j^2 represents the time-independent, variable-specific error terms. In the context of the Bayesian statistical inference, the posterior density of the parameters θ and the initial conditions of the sixteen state variables y_0 given the observed data y is defined as:

$$p(\theta, y_0, \sigma^2 | y) = \frac{p(y|f(\theta, x, y_0, \sigma^2))p(\theta)p(y_0)p(\sigma^2)}{\int \int p(y|f(\theta, x, y_0, \sigma^2))p(\theta)p(y_0)p(\sigma^2)d\theta dy_0 d\sigma^2} \propto p(y|f(\theta, x, y_0, \sigma^2))p(\theta)p(y_0)p(\sigma^2) \quad (3)$$

$p(\theta)$ is the prior density of the model parameters θ and $p(y_0)$ is the prior density of the initial conditions of the sixteen state variables y_0 . The characterization of the prior density $p(y_0)$ was based on the assumption of a Gaussian distribution with a mean value derived from the mid-winter monthly averages during the study period and standard deviation that was 25% of the mean value for each state variable j (Van Oijen et al., 2005); the prior densities $p(\sigma_j^2)$ were based on the conjugate inverse-gamma distribution (Gelman et al., 1995). Thus, the resulting posterior distribution for θ , y_0 , and σ^2 is:

$$p(\theta, y_0, \sigma^2 | y) \propto \prod_{j=1}^m (2\pi)^{-n/2} |\Sigma \delta_j|^{-1/2} \exp \left[-\frac{1}{2} [y_j - f_j(\theta, x, y_0)]^T \Sigma \delta_j^{-1} [y_j - f_j(\theta, x, y_0)] \right] \times (2\pi)^{-l/2} |\Sigma \theta|^{-1/2} \prod_{k=1}^l \frac{1}{\theta_k} \exp \left[-\frac{1}{2} [\log \theta - \theta_0]^T \Sigma \theta^{-1} [\log \theta - \theta_0] \right] \times (2\pi)^{-m/2} |\Sigma y_0|^{-1/2} \exp \left[-\frac{1}{2} [y_0 - y_{0m}]^T \Sigma y_0^{-1} [y_0 - y_{0m}] \right] \times \prod_{j=1}^m \frac{\beta_j^{\alpha_j}}{\Gamma(\alpha_j) \sigma_j^{2\alpha_j}} \exp \left(-\frac{\beta_j}{\sigma_j^2} \right) \quad (4)$$

where l is the number of the model parameters θ used for the model calibration ($l = 33$); θ_0 indicates the vector of the mean values of θ in logarithmic scale; $\Sigma \theta = I_l \times \sigma_\theta^T \times \sigma_\theta$ and $\sigma_\theta = [\sigma_{\theta 1}, \dots, \sigma_{\theta l}]^T$ corresponds to the vector of the shape parameters of the l lognormal distributions (standard deviation of $\log \theta$); the vector

$y_{0m} = [y_{1,1}, \dots, y_{1,16}]^T$ corresponds to the mid-winter values of the sixteen state variables; $\Sigma y_0 = I_m \times (0.25)^2 \times y_{0m}^T \times y_{0m}$; $\alpha_j (=0.001)$ and $\beta_j (=0.001)$ correspond to the shape and scale parameters of the m non-informative inverse-gamma distributions used in this analysis. Following the methodological protocol presented in our earlier modeling work (Arhonditsis et al., 2007, 2008a,b; Zhang and Arhonditsis, 2008), sequence of realizations from the posterior distribution of the model were obtained using Markov chain Monte Carlo (MCMC) simulations (Gilks et al., 1998; see also the relevant section in the Electronic Supplementary Material).

2.2.2. Prior parameter distributions

The calibration vector consists of the 33 most influential parameters as identified from an earlier sensitivity analysis of the model. The present analysis examines two different sets of priors aiming to assess the sensitivity of the posterior patterns on the assumptions made during the prior parameter specification, which has been an historical criticism of the Bayesian inference in the literature (Dennis, 1996; Ellison, 2004). The prior parameter distributions reflected the existing knowledge (field observations, laboratory studies, literature information and expert judgment) on the relative plausibility of their values. Specifically, the characterization of the parameter distributions was similar to the protocol used in Steinberg et al. (1997), i.e., we identified the minimum and maximum values for each parameter and then we assigned lognormal and loguniform distributions parameterized such that 99% (equal mass the two tail areas) and 100% of the respective values lay within the identified ranges. The delineation of the parameter spaces of the two phytoplankton functional groups was based on the framework presented in Zhang and Arhonditsis (2008). The prior distributions of all the parameters of the model calibration vector are presented in Table 1.

2.2.3. Model updating and loading scenarios

The MCMC estimates of the mean and standard deviation of the parameter values along with the covariance structure were used to update the model (Gelman et al., 1995). Under the multinormality assumption for the log transformed parameters, the mean values and the dispersion matrices of the conditional distributions were formulated as follows:

$$\hat{\theta}_{ij} = \hat{\theta}_i + [\hat{\theta}_j - \hat{\theta}_i] \Sigma_j^{-1} \Sigma_{ij} \quad (5)$$

$$\Sigma_{ij} = \Sigma_i - \Sigma_{ji} \Sigma_j^{-1} \Sigma_{ij} \quad j \in \{i+1, \dots, n\} \quad (6)$$

where $\hat{\theta}_{ij}$ and Σ_{ij} correspond to the mean value and the dispersion matrix of the parameter i conditional on the parameter vector j ; the values of the elements $\Sigma_i \Sigma_{ij}$

and Σ_j correspond to the variance and covariance of the two subsets of parameters; and $\hat{\theta}_i, \hat{\theta}_j$ correspond to the posterior mean and random values of the parameters i and j , respectively. The updated model provided the basis for a series of posterior simulations that aimed to reproduce the broad range of dynamics currently experienced in Hamilton Harbour or to determine the optimal nutrient loading reductions for achieving compliance with the targeted water quality standards.

In this study, we formulated probability distributions to accommodate the uncertainty as well as the interannual variability associated with the different exogenous nutrient loading sources in the Harbour (Fig. 4). Aside from the present loading conditions, we also examined three nutrient loading reduction strategies that all assumed a substantial reduction ($\approx 15\%$) of the non-point discharges into the system (Red Hill Creek, Grindstone Creek, and Cootes Paradise). The three scenarios also differed with regards to the point loadings examined, reflecting a gradual improvement in the performance of the Skyway and Woodward WWTPs. In particular, being the primary TP source in the area, the average loading from the Woodward WWTP was set equal to 194.2 kg day⁻¹, stemming from an approximate flow of 343 ML day⁻¹ and a concentration of 0.568 mg TP L⁻¹. The 2.5% and 97.5% uncertainty bounds of the TP loadings examined were 127.2 and 278.8 kg day⁻¹. The TP discharges from the same WWTP were reduced by 20% (to 155 kg day⁻¹) and 38% (to 120 kg day⁻¹) in scenarios 1 and 2, until set to the final goal of 60 kg day⁻¹ or 70% reduction as per the Hamilton Harbour RAP recommendations (HHTT-CLR, 2004). Similarly, the NH₄-N loadings from this source were reduced by 40% (to 1800 kg day⁻¹), 70% (to 900 kg day⁻¹), and 82% (to 530 kg day⁻¹) relative to the present levels (3023 kg day⁻¹), while the assumption of an equivalent NO₃ loading increase aims to represent the hypothetical scenario of enhanced nitrification in the WWTP. Cootes Paradise, a large wetland at the western end of the system, is another major nutrient loading source to the Hamilton Harbour. Beginning from an average of 40.8 kg day⁻¹, the TP loadings from Cootes were assumed to be reduced by 17% (to 34 kg TP day⁻¹) at the final HH RAP scenario. The role of the Burlington Skyway WWTP was examined assuming average loadings of 20.4 kg TP day⁻¹ and 155.9 kg NH₄-N day⁻¹ (present conditions), and ending up with 12 kg TP day⁻¹ and 115 kg NH₄-N day⁻¹ under the HH RAP proposition. The average TP loadings from Redhill and Grindstone Creeks varied from 22.2 to 15 kg TP day⁻¹ to 18.5 and 12.5 kg TP day⁻¹, respectively. Following the calculations of the HHTT-CLR (2004) report, we assumed an average loading of 52.7 kg TP day⁻¹ and 135.4 kg NH₄-N day⁻¹ (present conditions) from the combined sewer overflows, which was reduced by 91% (to 5 kg TP day⁻¹) and 85% (to 20 kg NH₄-N day⁻¹) in the final scenario [Specific details about the different nutrient loading scenarios are provided in the Electronic Supplementary Material].

Based on the previous probabilistic characterization of the external nutrient loading, we conducted 3000 posterior simulations to examine the exceedance

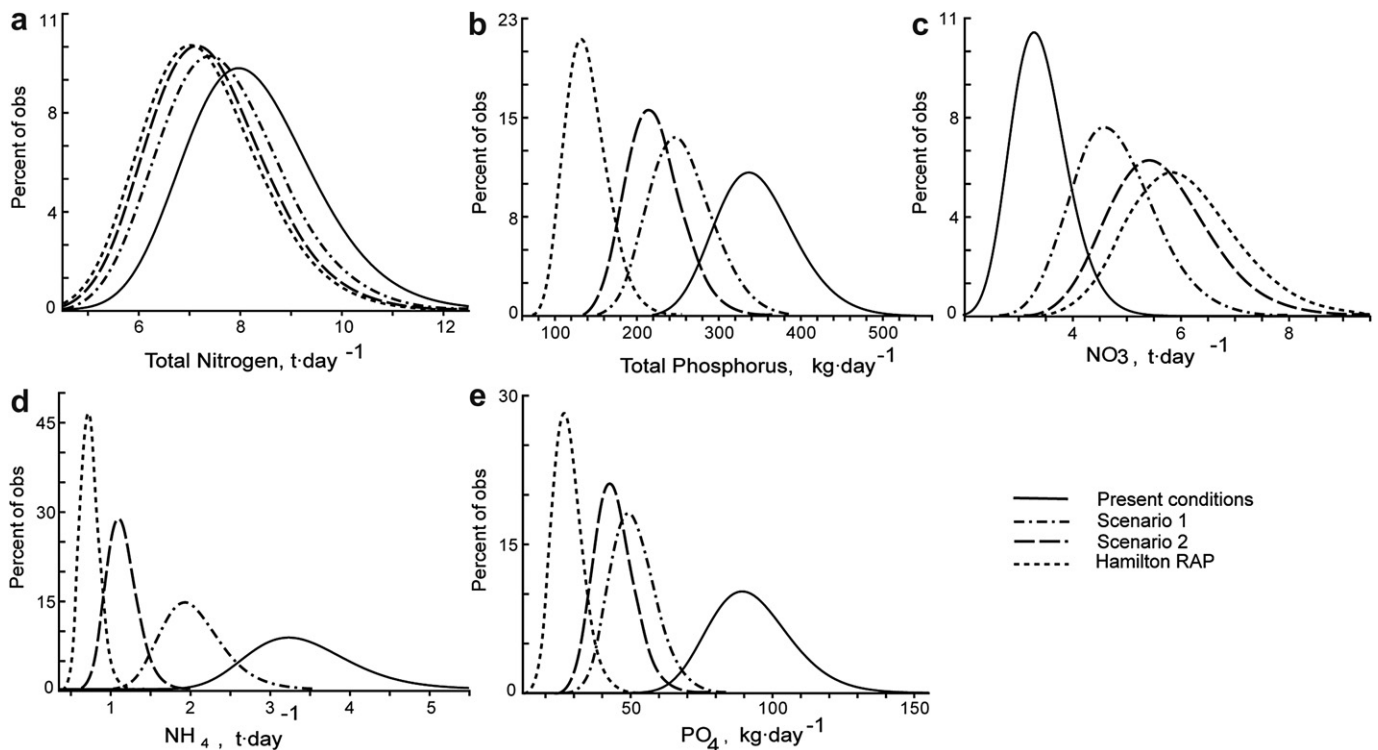


Fig. 4. Analysis of scenarios: Distributions of the total exogenous nutrient loadings used to force the Hamilton Harbour eutrophication model. Our analysis considers an average total loading of 8368 kg TN day⁻¹ and 351 kg TP day⁻¹ to represent the current conditions of the Harbour. The Hamilton Harbour RAP scenario implies a total loading of 7376 kg TN day⁻¹ and 142 kg TP day⁻¹. Scenarios 1 (7782 kg TN day⁻¹ and 260 kg TP day⁻¹) and scenario 2 (7552 kg TN day⁻¹ and 225 kg TP day⁻¹) depict two intermediate states that aim to assess the restoration rate of the system.

frequency of the Hamilton Harbour water quality standards ($10 \mu\text{g chl } a \text{ L}^{-1}$ and $17 \mu\text{g TP L}^{-1}$) under the present conditions and the three nutrient loading scenarios designed. For each iteration, we collected the weekly predicted values and the corresponding probabilities of exceeding the two water quality criteria (Zhang and Arhonditsis, 2008). The weekly predicted values along with the exceedance frequencies were then averaged over the summer stratified period (June–September). The distribution of these statistics across the posterior space was used to assess the expected exceedance frequency and the confidence of compliance with the two numerical criteria, while accounting for the uncertainty that stems from the model parameter uncertainty and the model error. We also note that the present analysis focuses on the average summer patterns and does not fully accommodate the day-to-day variability associated with the weather conditions and the interplay with Lake Ontario, which should be considered to improve the realism of our risk assessment statements.

3. Results

The two MCMC sequences of the model applications with the two sets of priors converged rapidly (≈ 5000 iterations) and the statistics reported were based on the last 35,000 draws by keeping every 20th iteration ($\text{thin} = 20$). The uncertainty underlying the values of the 33 model parameters after the MCMC sampling is depicted on the respective marginal posterior distributions (Table 1 and Fig. 5). Generally, the summary statistics of the posterior

parameter distributions indicate that substantial amount of knowledge was gained for the 33 parameters after the updating of the eutrophication model. Namely, several of the posteriors were characterized by significant shifts of their central tendency relative to the prior assigned values (e.g., $AH_{(\text{phyt})}$, $\text{filter}_{(\text{phyt})}$, $\text{filter}_{(\text{cy})}$, $kchl_{a(\text{phyt})}$, β_N , $\text{growthmax}_{(\text{cy})}$, V_{settling}), whereas the posterior standard deviations of the majority of the parameters were significantly lower than those specified prior to the calibration. Nonetheless, there were also model parameters with unaltered (e.g., $AH_{(\text{cy})}$, $kchl_{a(\text{cy})}$, $NH_{(\text{cy})}$, $NH_{(\text{phyt})}$, $PH_{(\text{cy})}$) or uninformative (e.g., bi/multimodal) posterior distributions (KZ , $PH_{(\text{phyt})}$, $P_{\text{maxuptake}_{(\text{phyt})}}$). We also highlight the robustness of the posterior patterns on the prior parameter specifications, as the discrepancy between the posterior means derived from the two sets of priors was lower than 20% for the vast majority of the parameters. Notable exceptions were the posterior standard deviations of the half saturation constant for phytoplankton ammonium uptake ($AH_{(\text{phyt})}$), the dreissenids filtering rate for phytoplankton ($\text{filter}_{(\text{phyt})}$), the cyanobacteria maximum growth rate ($\text{growthmax}_{(\text{cy})}$), the self-shading effects of the two phytoplankton groups ($kchl_{a(\text{cy})}$, $kchl_{a(\text{phyt})}$), the half saturation constant for nitrate cyanobacteria uptake ($NH_{(\text{cy})}$), and the two half saturation constants for phosphorus ($PH_{(\text{cy})}$, $PH_{(\text{phyt})}$).

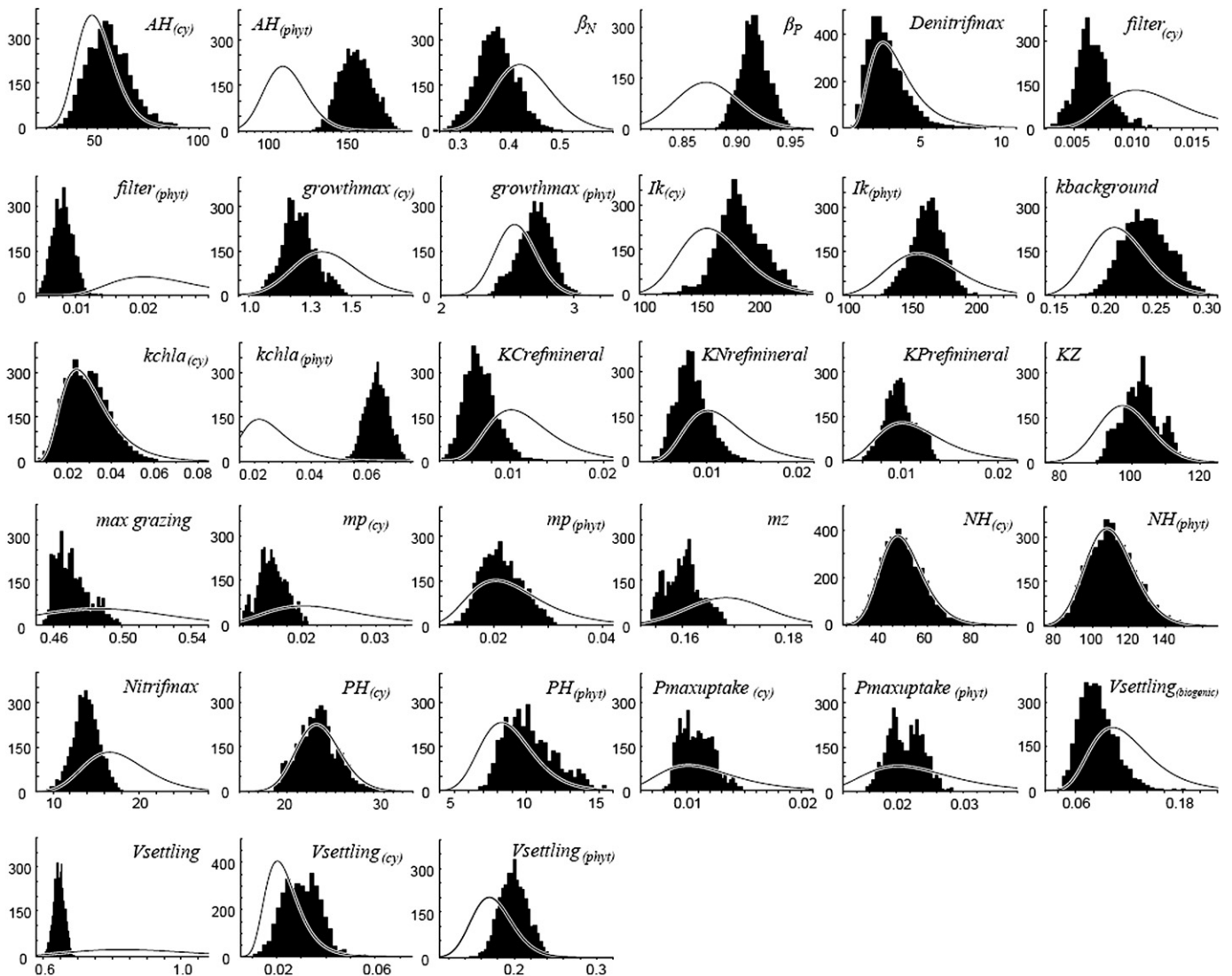


Fig. 5. Comparison between the prior (Lognormal) and posterior parameter distributions of the calibration vector of the Hamilton Harbour eutrophication model.

The seasonally invariant (model structure) error terms (σ_j) delineate constant zones around the model predictions for the 16 state variables (Table 2). The majority of the error terms were also remarkably similar between the two experiments with the different priors. The only notable relative differences were the somewhat higher error terms for the organic phosphorus and nitrate concentrations derived from the loguniform distributions.

The posterior medians along with the 95% credible intervals were fairly close to the observed values for phosphate, total phosphorus, ammonium, nitrate, total nitrogen, chlorophyll *a* and total zooplankton biomass in Hamilton Harbour (Fig. 6). In particular, the model accurately predicts the winter maxima ($\approx 11.5 \mu\text{g L}^{-1}$) and the summer minima ($\approx 2.2\text{--}4.7 \mu\text{g L}^{-1}$) of the epilimnetic phosphate levels as well as its hypolimnetic accumulation during the summer stratified period ($\approx 4.2\text{--}7.3 \mu\text{g L}^{-1}$). The model underpredicts somewhat the epilimnetic total phosphorus concentrations in autumn, which stems from the assumptions made regarding the intra-annual variability of the exogenous loading. The model closely reproduces the winter ($\approx 4.5 \mu\text{g chl } a \text{ L}^{-1}$) and the summer ($\approx 14 \mu\text{g chl } a \text{ L}^{-1}$) chlorophyll *a* levels, while the spring phytoplankton bloom is predicted to exceed the level of $20 \mu\text{g chl } a \text{ L}^{-1}$. Our model also predicts two major peaks of the zooplankton biomass; the first peak follows the spring phytoplankton bloom ($\approx 160 \mu\text{g C L}^{-1}$) while the second one is predicted to occur at the end of summer-mid fall ($\approx 200 \mu\text{g C L}^{-1}$). These predictions match closely the observed patterns reported by Dermott et al. (2007), e.g., Figs. 8 and 9; pages 62–63, if we assume an average wet to dry biomass ratio equal to 10 along with $0.4 \mu\text{g C}$ per μg of dry weight of zooplankton biomass (Downing and Rigler, 1984). The model performance was evaluated by three measures of fit: root mean squared error (RMSE), relative error (RE) and average error (AE) (Table 3). These comparisons aimed to assess the goodness-of-fit between the means of the predictive distributions and the observed values. The highest RE values were found for the volume weighted zooplankton biomass (45.40%), the epilimnetic phosphate (32.80%), and the epilimnetic chlorophyll *a* concentrations (27.25%). We also highlight the fairly low RE values for nitrate (3.05%), total nitrogen (4.60%), and both the epilimnetic (9.71%) and hypolimnetic (6.95%) total phosphorus concentrations. The average error is a measure of aggregate model bias, though values near zero can be misleading because negative and positive discrepancies can cancel each other. In most cases, we found that the means of the predictive distributions do not introduce systematic bias, although two notable exceptions were the

overestimation of the zooplankton biomass and epilimnetic chlorophyll *a* concentrations with AE values of $8.41 \mu\text{g C L}^{-1}$, and $1.58 \mu\text{g chl } a \text{ L}^{-1}$, respectively. The root mean square error is another measure of the model prediction accuracy that overcomes the shortcoming of the average error by considering the magnitude rather than the direction of each difference. The RMSE for the zooplankton and phytoplankton biomass were $54.77 \mu\text{g C L}^{-1}$ and $3.95 \mu\text{g chl } a \text{ L}^{-1}$, respectively. We also note the approximately 4.00 and $3.14 \mu\text{g TP L}^{-1}$ mean discrepancy between the predictive means and the observed epilimnetic and hypolimnetic total phosphorus concentrations.

The model predicts that the current average TP and chlorophyll *a* concentrations are $28.62 \pm 3.15 \mu\text{g L}^{-1}$ and $14.85 \pm 1.44 \mu\text{g chl } a \text{ L}^{-1}$ during the summer stratified period, while the associated distributions lie well above the existing water quality criteria of $17 \mu\text{g TP L}^{-1}$ and $10 \mu\text{g chl } a \text{ L}^{-1}$ (Fig. 7). The reduction of the total TP loading by approximately 25% ($260 \pm 40 \text{ kg day}^{-1}$) does substantially improve the water quality conditions but does not result in an attainment of the targeted goals. Specifically, the average summer TP and chlorophyll *a* concentrations were $22.73 \pm 2.59 \mu\text{g L}^{-1}$ and $12.89 \pm 1.14 \mu\text{g chl } a \text{ L}^{-1}$. Likewise, an additional reduction to the level of $225 \pm 35 \text{ kg TP day}^{-1}$, will primarily decrease the summer TP concentration ($20.42 \pm 2.27 \mu\text{g L}^{-1}$) and secondarily the chlorophyll *a* levels ($12.25 \pm 1.04 \mu\text{g chl } a \text{ L}^{-1}$), although the system will still not comply with the water quality standards. The implementation of the HH RAP loading propositions suggests that the projected average summer 10% concentrations ($14.38 \pm 1.86 \mu\text{g L}^{-1}$) will fall below the $17 \mu\text{g TP L}^{-1}$ threshold value, while the corresponding exceedance frequency will be about 13.8%. If we follow strictly the RAP guidelines (i.e., $\text{TP} < 17 \mu\text{g L}^{-1}$ throughout the June–September period), the latter prediction is still reflective of non-compliance of the system. However, the adoption of a TP criterion that permits a prespecified level of violations (e.g., $\leq 10\%$ exceedance in space and time), may be a more realistic assessment of the anticipated water quality conditions as it accommodates both natural variability and measurement/sampling error. For example, the proportion of the exceedance frequency distribution that lies below the 10% cutoff point (or confidence of compliance with the TP standard) is more than 75%, suggesting that this water quality criterion is likely to be met if the HH RAP recommendations are adopted (Fig. 8). By contrast, the average chlorophyll *a* concentration is predicted to be $10.38 \pm 0.88 \mu\text{g L}^{-1}$ with $>50\%$ probability of exceeding the $10 \mu\text{g chl } a \text{ L}^{-1}$ value. Consequently, our confidence of compliance with the same threshold level is less than 10%, and therefore it is nearly impossible to comply with the 10% EPA guideline. Yet, despite the fact that chlorophyll *a* is not predicted to meet the $10 \mu\text{g L}^{-1}$ target, the conditions in the Harbour are still expected to improve the water clarity or to decrease the biogenic sedimentation which in turn could potentially improve hypolimnetic DO levels.

4. Discussion

We used a Bayesian modeling framework to obtain a good representation of several key water quality variables (chlorophyll *a*, total zooplankton biomass, phosphate, and total phosphorus) in Hamilton Harbour. This framework was also used to estimate the critical nutrient loads that will ultimately result in acceptable exceedance frequencies and appropriate margins of safety with the existing water quality criteria. While none of the water quality goals is currently accomplished, our analysis suggests that the epilimnetic TP concentrations will decrease in response to a reduction in external nutrient loadings and that the water quality goal of $17 \mu\text{g TP L}^{-1}$ will likely be met (confidence of compliance $\approx 80\%$), if the Hamilton Harbour RAP proposition for phosphorus loading at

Table 2
Markov Chain Monte Carlo posterior estimates of the mean values and standard deviations of the model structure error terms.

Parameters	Loguniform		Lognormal	
	Mean	Std. Dev.	Mean	Std. Dev.
$\sigma_{\text{PO}_4\text{epi}}$	0.396	0.131	0.389	0.131
σ_{OPepi}	1.301	0.315	1.148	0.271
$\sigma_{\text{NH}_4\text{epi}}$	52.23	12.26	50.02	11.99
$\sigma_{\text{NO}_3\text{epi}}$	172.3	40.48	159.4	38.64
σ_{ONepi}	7.503	1.921	7.654	1.864
σ_{CYAepi}	1.277	0.449	1.244	0.469
σ_{PHYTepi}	25.28	7.728	22.82	7.363
σ_{ZOOepi}	5.601	1.792	5.709	1.922
$\sigma_{\text{PO}_4\text{hypo}}$	0.625	0.169	0.742	0.198
σ_{OPhypo}	1.515	0.374	1.231	0.323
$\sigma_{\text{NH}_4\text{hypo}}$	29.76	8.886	29.14	8.943
$\sigma_{\text{NO}_3\text{hypo}}$	196.8	47.08	180.9	44.99
σ_{ONhypo}	12.28	3.049	11.99	2.845
σ_{CYAhypo}	3.157	0.767	3.363	0.824
σ_{PHYThypo}	45.15	11.48	49.07	12.16
σ_{ZOOPhypo}	6.128	1.393	6.205	1.449

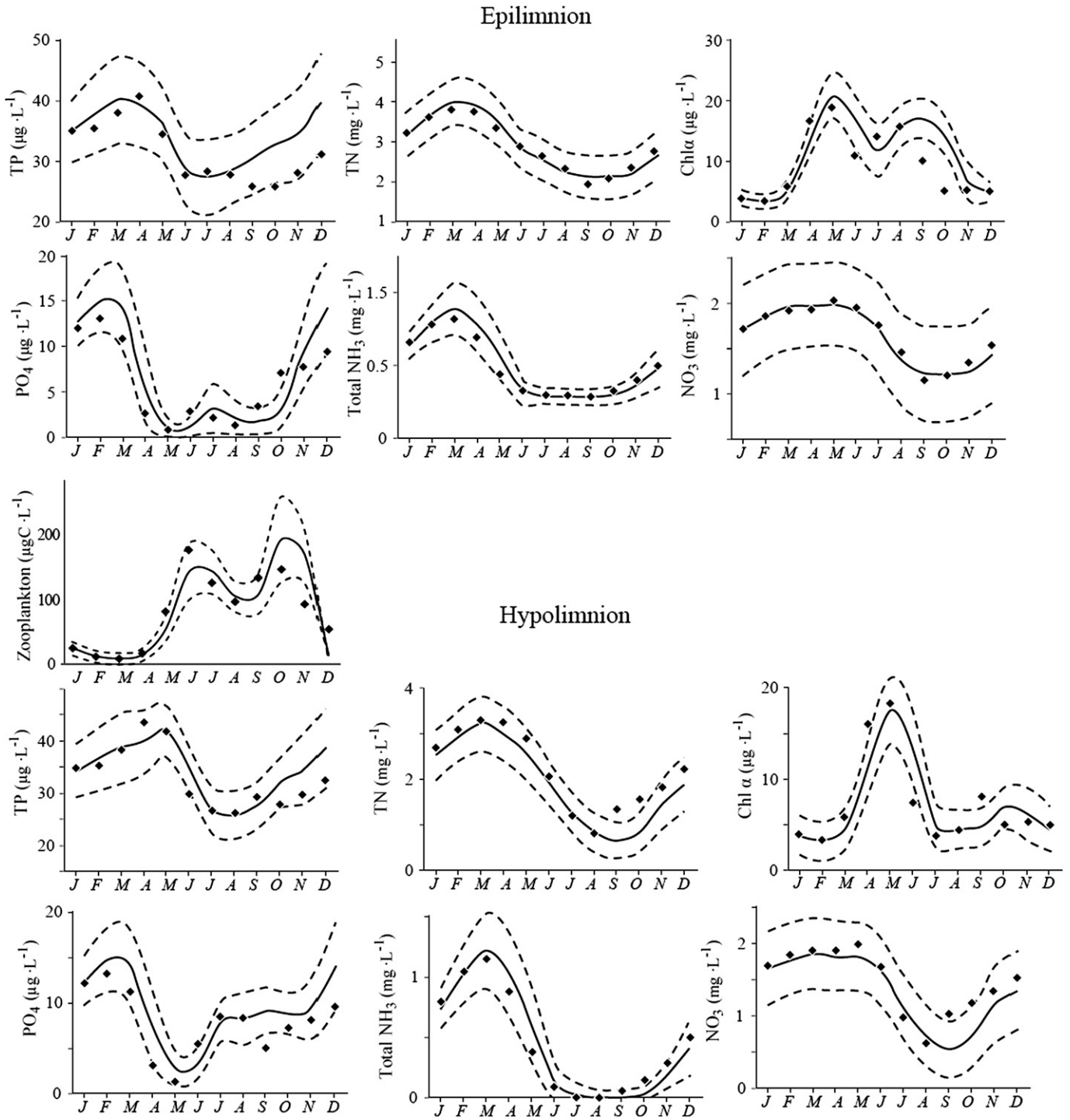


Fig. 6. Comparison between the observed data (black dots) and the mean predictions for total phosphorus, total nitrogen, chlorophyll *a*, phosphate, ammonium, nitrate, and total zooplankton biomass in the Hamilton Harbour epilimnion and hypolimnion. The credible intervals represent the uncertainty pertaining to the model parameters and structure along with the variability characterizing the exogenous nutrient loading.

the level of 142 kg day^{-1} is achieved. The attainment of the water quality goal related to the summer chlorophyll *a* concentrations ($5\text{--}10 \mu\text{g L}^{-1}$) though has not been unequivocally demonstrated, as the central tendency of our predictions indicates a marginal exceedance of the $10 \mu\text{g L}^{-1}$ threshold level, even when the exogenous loading conforms to the most extreme reduction guidelines. The projected disconnect between the TP and chlorophyll *a* standards invites critical reassessment of the stressor–effect

relationships historically used in the Harbour as well as identification of the factors unaccounted for by our modeling exercise that can potentially modulate the anticipated system responses to the exogenous nutrient loading reductions designed.

The relationship of the epilimnetic summer TP with the total TP loading to the Harbour is characterized by an increase in the slope between the present conditions ($\text{TP}_{\text{Harbour}} = 0.055 \times \text{TP}_{\text{Loading}} + 7.343$) and the HH RAP scenario ($\text{TP}_{\text{Harbour}} = 0.064 \times \text{TP}_{\text{Loading}} + 5.272$), which

Table 3
Goodness-of-fit statistics for the epilimnetic and hypolimnetic model predictions.^a

State variables	Epilimnion			Hypolimnion		
	RMSE	RE	AE	RMSE	RE	AE
Chlorophyll <i>a</i> biomass ($\mu\text{g chl } a/\text{L}$)	3.948	27.25%	1.581	2.607	24.47%	-0.077
Ammonium (mg N/L)	0.102	15.79%	0.025	0.099	17.85%	0.010
Nitrate (mg N/L)	0.059	3.05%	-0.016	0.226	11.44%	-0.130
Phosphate ($\mu\text{g P/L}$)	2.484	32.80%	0.841	2.496	26.04%	1.558
Total Nitrogen (mg N/L)	0.126	4.60%	0.039	0.346	12.52%	-0.254
Total Phosphorus ($\mu\text{g P/L}$)	4.000	9.71%	2.650	3.145	6.95%	1.201
Total Zooplankton biomass ($\mu\text{g C/L}$)	54.77	45.40%	8.408			

^a RMSE – Root Mean Square Error; RE – Relative Error; AE – Average Error.

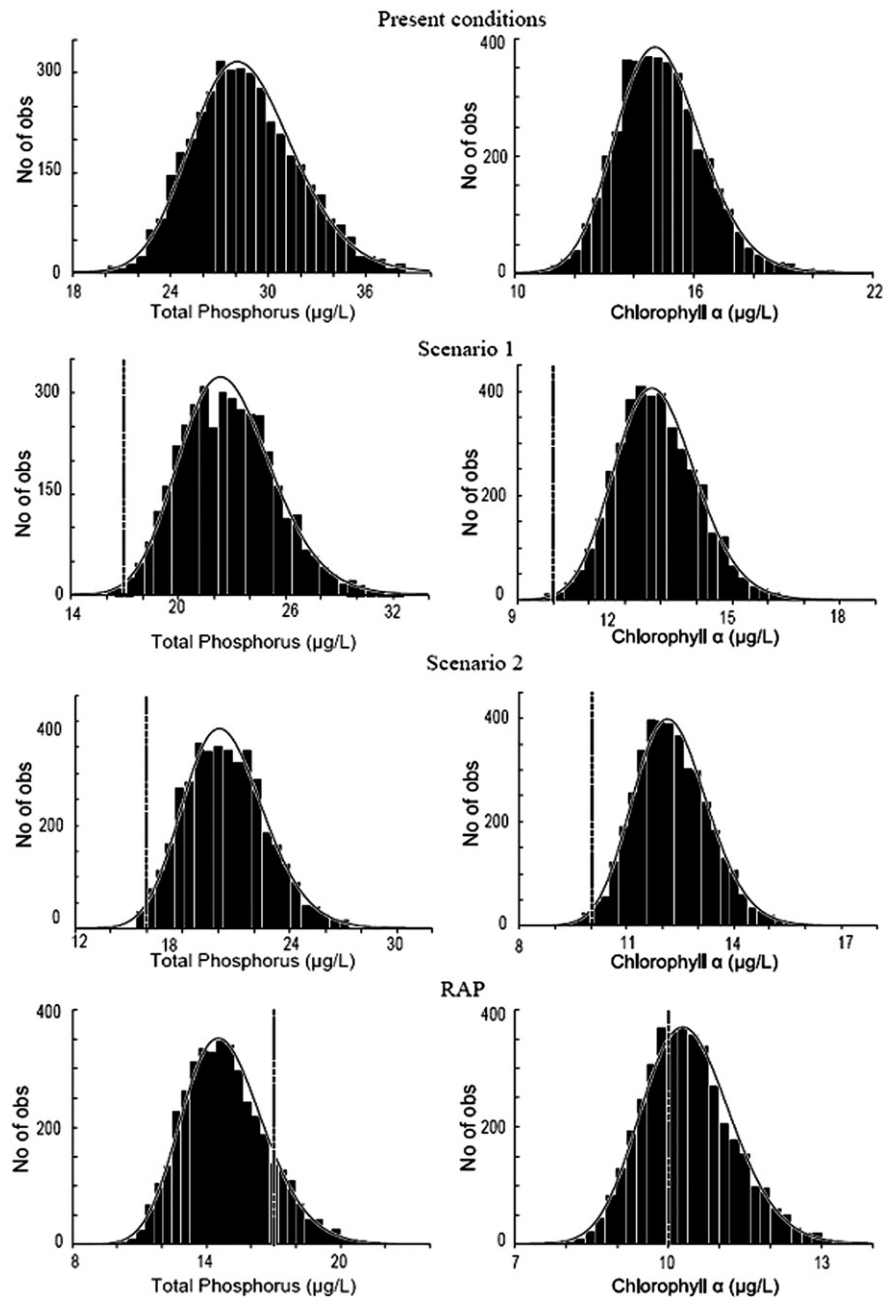


Fig. 7. Marginal predictive distributions of total phosphorus and chlorophyll *a* during the summer stratified period in Hamilton Harbour under the four nutrient loading scenarios examined.

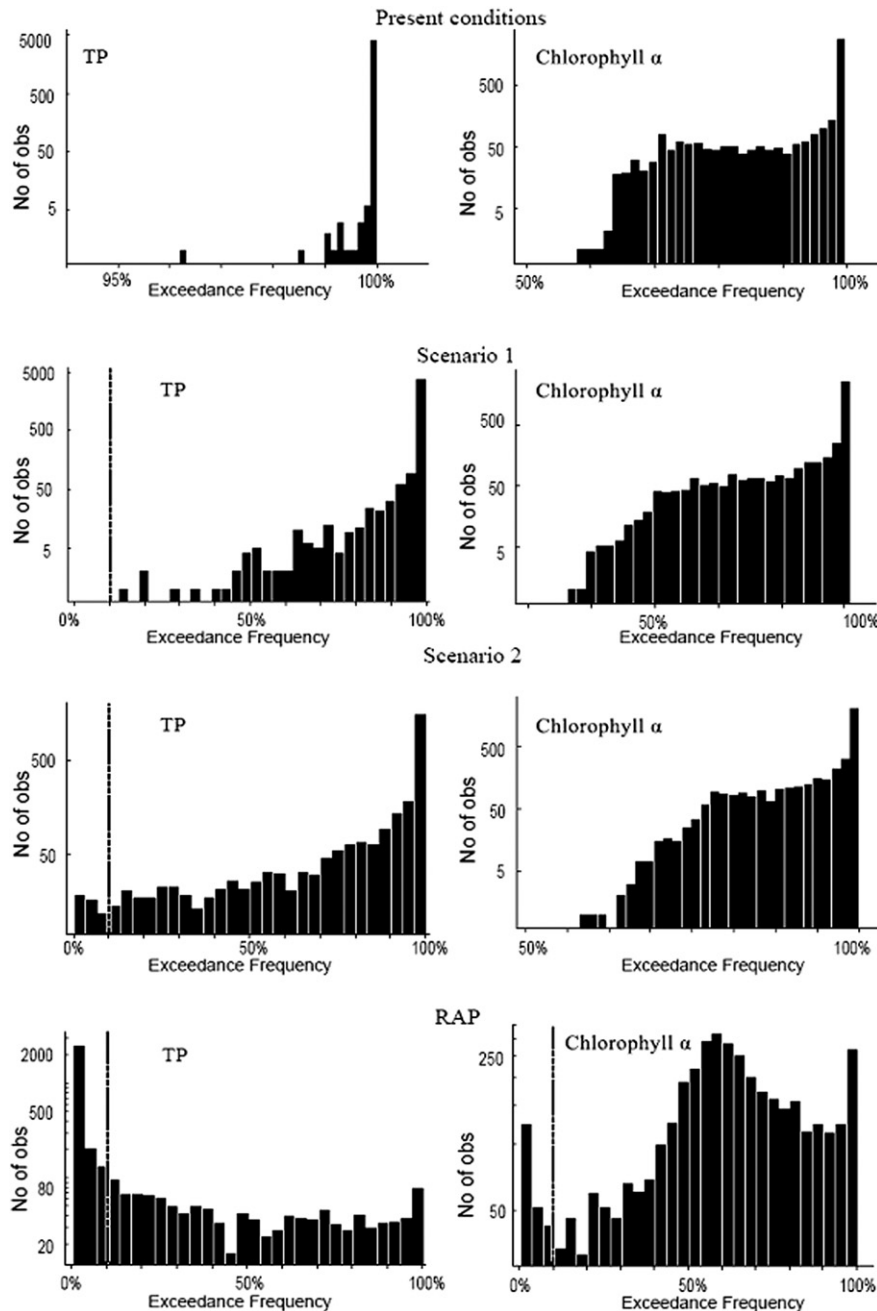


Fig. 8. Exceedance frequency of the total phosphorus ($17 \mu\text{g L}^{-1}$) and chlorophyll a ($10 \mu\text{g L}^{-1}$) water quality standards during the summer stratified period in Hamilton Harbour. These distributions represent the probabilities of the predicted exceedance frequencies, and assess the degree of confidence that the true value of the violation frequency is below a specified value. The area below the 10% cutoff point is termed the confidence of compliance, showing the probability that the true exceedance frequency is below the 10% EPA guideline.

suggests a somewhat tighter coupling between the ambient Harbour conditions and the exogenous nutrient loadings (Fig. 9a). The $\text{TP}_{\text{Harbour}}$ predictions of our linear regression equations are lower than those supported by the iron-modified Janus–Vollenweider relationship used for setting the TP numerical criterion in Hamilton Harbour (Charlton, 2001). Namely, our analysis suggests ambient TP concentrations lower than $20 \mu\text{g L}^{-1}$ at a critical loading level of $200 \text{ kg TP day}^{-1}$, while the Janus–Vollenweider empirical approach supported predictions of $23 \mu\text{g TP L}^{-1}$. A plausible explanation for this discrepancy is that, while both models account for iron-induced phosphorus precipitation to the bottom sediments, they do not share the same application domain as our equations refer to the summer TP average instead of the annual TP levels. The

$\text{chl } a_{\text{Harbour}}\text{--TP}_{\text{Loading}}$ regression equations derived from our Monte Carlo analysis (Present conditions: $\text{chl } a_{\text{Harbour}} = 0.013 \times \text{TP}_{\text{Loading}} + 9.688$; HH RAP: $\text{chl } a_{\text{Harbour}} = 0.024 \times \text{TP}_{\text{Loading}} + 6.795$) support predictions of lower average summer chlorophyll a concentrations, and therefore appear to correct the systematic bias found from the applications of the Chapra and Dobson (1981) and Dillon and Rigler (1974) models in Hamilton Harbour (Fig. 9b). Specifically, our analysis suggests an approximate value of $13 \mu\text{g chl } a \text{ L}^{-1}$ at a loading level of 200 kg day^{-1} , whereas the corresponding predictions of the two empirical models are $18 \mu\text{g chl } a \text{ L}^{-1}$ and $28 \mu\text{g chl } a \text{ L}^{-1}$ [The latter prediction stems from the Dillon and Rigler, 1974 model and refers to the maximum summer chlorophyll a concentrations]. Thus, relative to the existing $\text{chl } a_{\text{Harbour}}$ or $\text{TP}_{\text{Harbour}}\text{--TP}_{\text{Loading}}$ relationships, our

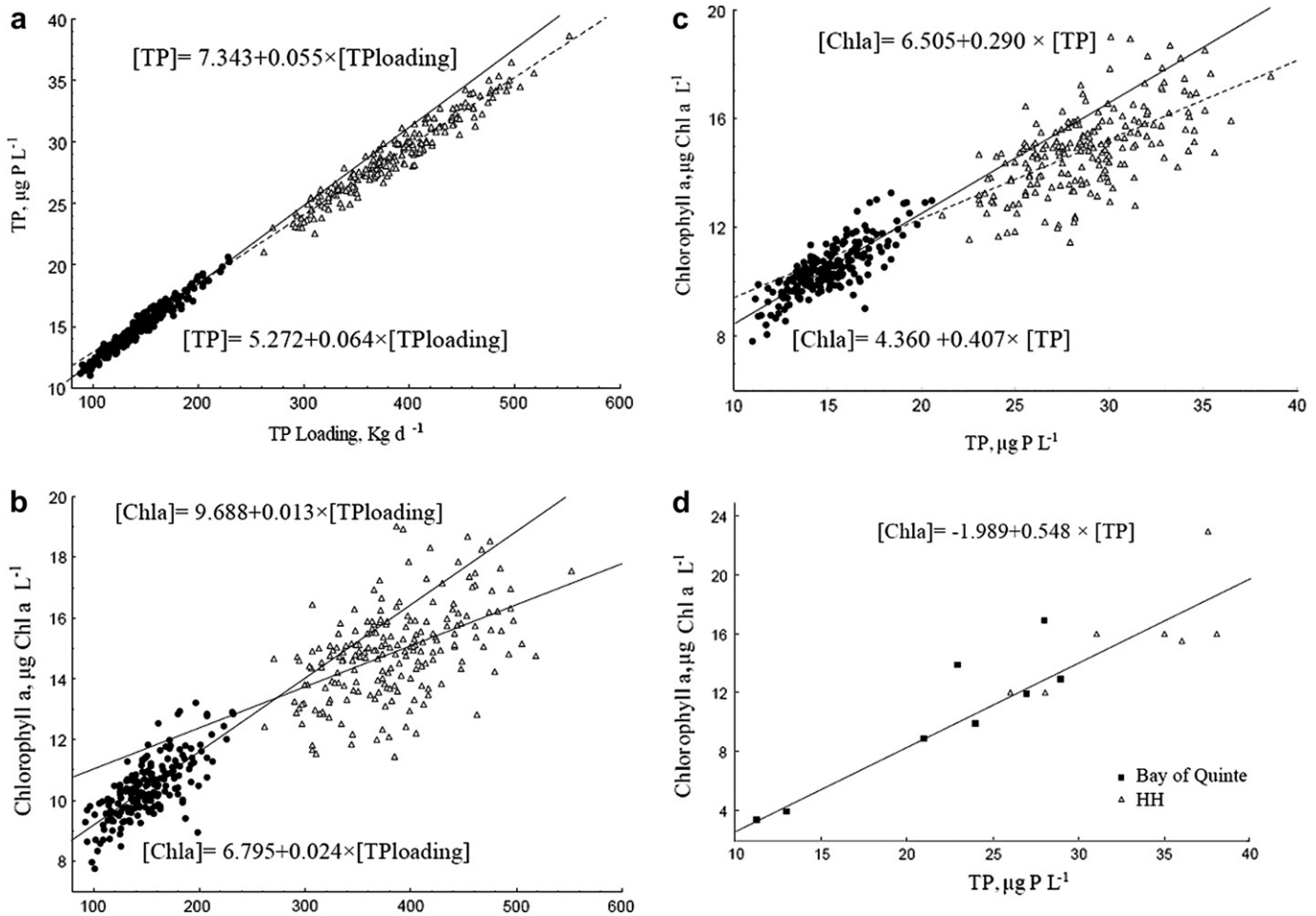


Fig. 9. Analysis of scenarios: Relationships between chlorophyll *a*, total phosphorus and TP loading in Hamilton Harbour based on the present nutrient loading conditions and the HH RAP propositions. The fourth panel illustrates the mean summer total phosphorus versus chlorophyll *a* concentrations for Hamilton Harbour and the Bay of Quinte (2002–2004), as adapted from the Dermott et al. (2007) study.

analysis predicts a more abrupt decline in the TP and chl *a* concentrations with a concomitant decrease in TP loading. Bearing in mind though that all the earlier empirical models were founded upon a systematic underestimation of the loadings from the Woodward WWTP up to the year 2000, we emphasize that the accuracy of our projections is contingent upon the credibility of the contemporary nutrient loading estimates in the Harbour. In particular, the piecewise monotonically increasing approach to the nutrient concentrations versus flow patterns typically used to estimate the nutrient loadings from episodic precipitation events is not substantiated by the recent data (HHTT-CLR, 2004; Gudimov et al., 2010). Another key assumption made to derive the nutrient loading estimates from Cootes Paradise is that the flows into the system equal the outflows into the Harbour. The validity of this practice has been challenged as it may underestimate the discharges due to diffusive mixing driven by the gradients in the water quality characteristics and/or the lake seiches (HHTT-CLR, 2004). The Cootes Paradise is a highly productive system with high chl *a* ($>30 \mu\text{g L}^{-1}$) and TP ($>50 \mu\text{g L}^{-1}$) concentrations (Chow-Fraser et al., 1998). Our model does not explicitly consider either the amount or the composition (relative cyanobacteria abundance) of the phytoplankton biomass exported from Cootes, postulating that the impact to the Harbour is minimal (Hiriart-Baer et al., 2009); the implications of this assumption will be investigated in subsequent analysis.

The chl *a*–TP relationships derived from our analysis suggest a stronger association between the two water quality variables as we shift from the present loading conditions (chl $a = 0.290 \times TP + 6.505$) to the HH RAP propositions (chl

$a = 0.407 \times TP + 4.360$) (Fig. 9c). Furthermore, given that other factors beyond nutrients can limit primary production, we characterized the phosphorus limitation status of the simulated environments using as a proxy the chl *a*: particulate phosphorus (PP) ratio. Following Hiriart-Baer et al.'s (2009) approach, Monte Carlo samples with chl *a*:PP ratios <0.8 were categorized as phosphorus sufficient and those with ratios ≥ 0.8 were categorized as phosphorus limited. The model predicts that P-limited algae occur in the system under the present loading conditions, but the frequency of the P-limited runs was lower than 5% of the total MC samples generated. Our analysis also shows that an average TP loading of 142 kg day^{-1} will establish a strongly phosphorus-limiting environment ($>90\%$ of the model runs sampled), although the prediction of our regression equation ($\approx 11.2 \mu\text{g chl a L}^{-1}$) at an average TP level of $17 \mu\text{g L}^{-1}$ is higher than the targeted value of $10 \mu\text{g chl a L}^{-1}$. Among the existing chl *a*–TP relationships reported in the literature, our results are relatively close to the trajectory delineated by Hiriart-Baer et al. (2009) using data classified as P-limited (see their Fig. 6). However, the similarities drawn from this comparison should be interpreted with caution for two basic reasons: (i) the Hiriart-Baer et al. (2009) study is based on data from individual samplings (snapshots) rather than seasonal means; and (ii) the targeted chl *a* ($<10 \mu\text{g L}^{-1}$) vs TP ($<17 \mu\text{g L}^{-1}$) region represents the lower end of the application domain of their relationship. Our results also differ from the Burley (2007) projection, which suggests that the summer chlorophyll *a* averages will be lower than

$10 \mu\text{g L}^{-1}$ with summer TP levels below the $20 \mu\text{g L}^{-1}$ level (see adapted graph in Fig. 9d). Notably, the form of this line (slope and intercept) is driven by three potentially influential points (i.e., high leverage values) corresponding to seasonal means from the Bay of Quinte; a Z-shaped system on the northeastern shore of Lake Ontario (Millard and Sager, 1994). Hence, an important question that arises is to what extent we can put the present projections into perspective by drawing parallels between the two Areas of Concern? A direct comparison of the two systems with regards to their circulation patterns, nutrient dynamics, and food web structure may offer meaningful insights into the anticipated responses of the Harbour.

Given the lack of reliable information to assess the plausibility of our projections, we believe that it is also critical to invoke the role of other potentially important factors in modulating the phytoplankton response to the variability of the ambient TP levels, such as the control exerted from the zooplankton community, internal loading, and filtration from the invasive zebra and quagga mussels. The strong connection between algal concentrations and zooplankton biomass in Hamilton Harbour was observed especially in 1997, when the prolonged and unusually high zooplankton abundance resulted in Secchi depth measurements of greater than 5 m (Charlton, 2001). The zooplankton community in its present state still indicates that Hamilton Harbour is eutrophic, being dominated by cladocerans and cyclopoids (*Diacyclops thomasi*, *Cyclops vernalis*) compared to calanoids (*Leptodiatomus siciloides*) (Gerlofsma et al., 2007). Cladocerans mainly include the *Bosmina longirostris*, species from the *Daphnia* and *Ceriodaphnia* genera, and the carnivorous species *Leptodora kindtii* and *Cercopagis pengoi*. While the present model structure does not explicitly consider the functional role of the different taxonomic groups, the parameterization of our generic “zooplankton” variable can offer insights into the optimal features of the mean zooplankton community to effectively advance the transition of the Harbour from the present eutrophic to a mesotrophic state. For example, the examination of different zooplankton configurations (maximum grazing rates, half saturation constant for grazing, zooplanktivory levels) vis-à-vis nutrient loading conditions with the updated model suggests a non-linear response of the chl *a*–TP levels to the zooplankton biomass variability (Fig. 10a). Specifically, the chlorophyll *a* concentrations as well as the slope of the chl *a*–TP relationship increase dramatically when the mean summer zooplankton abundance drops below an approximate level of $100 \mu\text{g C L}^{-1}$ (or $2500 \mu\text{g wet weight L}^{-1}$). Although this threshold value is somewhat lower than the current average summer levels in the system, it does highlight the critical role of herbivory in attaining the chl *a* criterion and also invites further investigation of the factors that could potentially control the trajectory of the zooplankton community as we gradually shift to a reduced nutrient loading regime (Gudimov et al., 2010).

Given the absence of an explicit third trophic level from the model, the zooplankton mortality parameter effectively acts as surrogate term for the top-down control in the system and our analysis shows that the so-called closure term can significantly alter the standing phytoplankton biomass, e.g., $5\text{--}12 \mu\text{g chl } a \text{ L}^{-1}$ at $17 \mu\text{g TP L}^{-1}$ (Fig. 10b). In particular, our calibration exercise approximately allocates 16% of the herbivorous zooplankton biomass to support the upper trophic levels on a daily basis, i.e., the posterior probability of the parameter *mz* extends over the $0.15\text{--}0.17 \text{ day}^{-1}$ range. Consistent with our model parameterization, empirical evidence stresses the relatively high intensity of zooplanktivory in the system. For example, Gerlofsma et al. (2007) reported relatively high chlorophyll *a*/total phosphorus ratios ($0.41\text{--}0.62$) in the Harbour, which were interpreted as evidence of an odd-link system characterized by strong predation of

zooplankton by fish (Mazumder, 1994). Supportive of the latter assertion was also deemed the smaller mean length of cladocerans ($320\text{--}425 \mu\text{m}$) in the Harbour relative to the Bay of Quinte (Gerlofsma et al., 2007; see their Fig. 7 in pg 88), considering that fish preferentially consume larger zooplankton individuals and the mean zooplankton community length can reflect the balance between piscivores and planktivores within the fish community (Mills et al., 1987). The current fish community is mainly dominated by benthivores such as brown bullhead (*Ameiurus nebulosus*), carp (*Cyprinus carpio*), and white perch (*Morone americana*), and planktivores such as alewife (*Alosa pseudoharengus*), and gizzard shad (*Dorosoma cepedianum*). These species thrive under low dissolved oxygen conditions and high suspended solid concentrations, while their feeding and spawning activities uproot vegetation and stir up bottom sediments (Scheffer and van Nes, 2004). The predominance of these pollution-tolerant species has consequently kept many desirable fish species at low levels, such as northern pike (*Esox lucius*), largemouth bass (*Micropterus salmoides*), and walleye (*Sander vitreus*), while the role of the dominant piscivore in the system has been assumed by the (more adaptable in polluted habitats) channel catfish (*Ictalurus punctatus*). Acknowledging the dire repercussions of the fish community structural shifts on the ecosystem integrity (including the degradation of zooplankton), the Hamilton Harbour RAP (1992) outlined multiple remedial actions (restoration of destroyed or preservation of existing habitats, control of undesirable and introduction of desired species) aiming to restore the piscivorous populations and bring the fish community as close as possible to the historical norms. While the success of the fish restoration efforts has been traditionally perceived as being dependent upon the water quality improvements, we argue that the two management actions at this stage should rather be viewed as having a recursive relationship that will likely modulate the restoration rate as well as the stability of the new trophic state in the Harbour. A characteristic example of the latter point is the Lake Washington case, where an unexpected event (the elimination of the shrimp *Neomysis mercedis* from a thriving longfin smelt population) allowed the resurgence of *Daphnia* and subsequently stabilized the mesotrophic state in the system (Edmondson, 1994; Arhonditsis et al., 2004).

Aside from the critical role of planktivory, our analysis also predicts that a fast growing zooplankton community characterized by grazing rate greater than 0.6 day^{-1} and half saturation constant lower than $100 \mu\text{g C L}^{-1}$ should minimize the exceedances of the $10 \mu\text{g chl } a \text{ L}^{-1}$ criterion when the $17 \mu\text{g TP L}^{-1}$ level is achieved (Fig. 10c, d). Following Gerlofsma et al.'s (2007) proposition, the feeding kinetics derived from this exercise could be potentially associated with the size or length of the zooplankters to determine the optimum zooplankton composition in the Harbour (Johannsson et al., 2000). We also emphasize one more unresolved issue with regards to the zooplankton feeding patterns. In our model, because of the absence of reliable estimates of exogenous particulate carbon loadings, we did not explicitly consider the carbon cycle and therefore the zooplankton diet exclusively depends on endogenous sources (algae and detritus). While recent studies render support to our approach downplaying the role of allochthony (Brett et al., 2009), this feature of the model should be revisited in future refinements as it may unrealistically strengthen the coupling of the phytoplankton–zooplankton relationship in the Harbour. For example, Munawar and Fitzpatrick (2007) argued that the high proportion of secondary to primary producers observed in Hamilton Harbour is evidence that the autochthonous production may not likely be sufficient to sustain the food web. Consequently, the same study hypothesized that other sources of autochthonous (benthic algae and macrophytes) and allochthonous energy may be equally important. The quantification of the relative support of

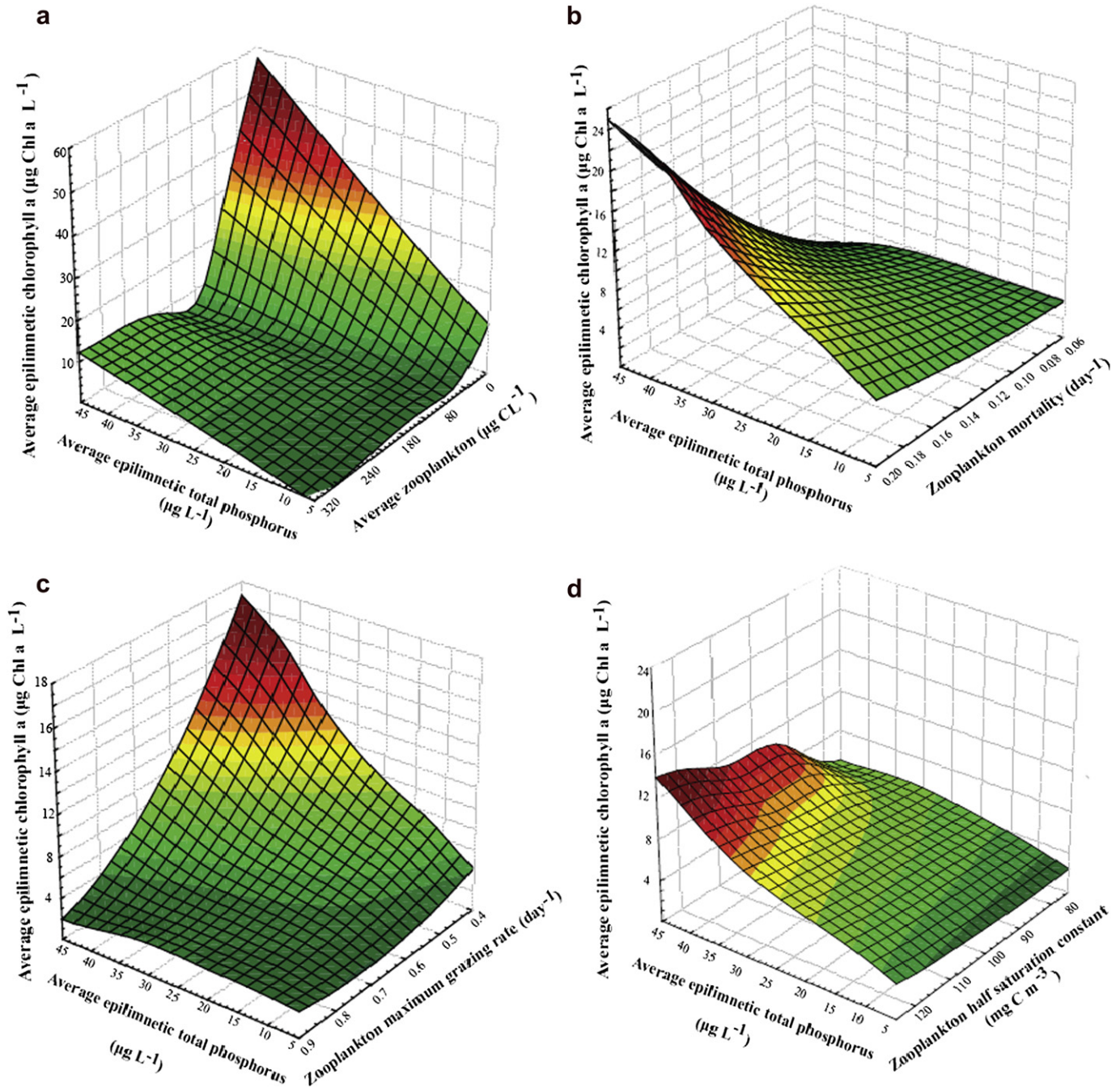


Fig. 10. Examination of the top-down control in attaining the chlorophyll a water quality goals.

consumers by autochthonous vis-à-vis allochthonous resources may be pivotal in projecting the response of planktonic communities to the expected changes of the ambient nutrient levels (Gudimov et al., 2010). Given that the gradual decrease of the biogenic material should likely induce shifts in zooplankton's diet, the question that arises is to what extent the increased reliance upon exogenous sources can pose threats to the integrity of the zooplankton community in the system?

Another important regulatory factor of the phytoplankton biomass response to the reduction of the exogenous nutrient loadings could have been the abundance of the invasive zebra and quagga mussels. Several field studies in the Great Lakes have reported changes in phytoplankton community structure after

zebra mussel invasions (e.g., Smith et al., 1998; Budd et al., 2001; Nicholls et al., 2002). Zebra mussels can affect phytoplankton biomass, productivity and community structure through non-selective filtration and removal of suspended particles from the water column (Maclsaac et al., 1992; Fahnenstiel et al., 1995; James et al., 1997), selective rejection of certain types of ingested algae (Makarewicz et al., 1999; Vanderploeg et al., 2001), and excretion of soluble forms of nutrients by mussels (Effler et al., 1997; Canale and Chapra, 2002; Bierman et al., 2005). In this study, consistent with existing evidence from the system, the posterior distributions of the corresponding parameters $filter_i$, downplay the role of dreissenids in the Harbour. Aside from the nearshore zones, Hamilton Harbour is one of the few shallow Great Lakes systems where

dreissenids are not abundant, and the unsuitable, soft bottomed habitat beyond 8 m has limited the average biomass to about one-tenth of the densities experienced in Lake Erie and the Bay of Quinte (Dermott and Bonnell, 2007). Other factors that may constrain their proliferation include the summer anoxia of the hypolimnion that does not allow the dreissenids to survive in the middle of the Harbour, and the elevated Cr, Cu, Hg, Pb, and Zn sediment concentrations that can reduce survival and induce strong genotoxic responses (Munawar et al., 1999; Marvin et al., 2000). While some improvement in surficial sediment quality is expected following the wastewater and storm drain management actions, the continuing anoxic conditions and the re-suspension of historically-contaminated sediment from shipping and storm disturbance will likely preclude major dreissenid-induced planktonic food web alterations in the central part of the Harbour (Rukavina and Versteeg, 1996).

Hamilton Harbour also experiences a significant hypolimnetic dissolved oxygen deficit during the stratification period, and its severity is primarily determined by the thickness of the hypolimnion along with the hydraulic exchanges with Lake Ontario (Barica, 1989; Hiriart-Baer et al., 2009). Aside from these natural factors, the anthropogenic nutrient inputs exacerbate the problem by increasing the chemical (nitrification) and biological (organic matter decomposition) oxygen-demanding processes in the Harbour. In our analysis, the posterior values obtained for the parameter β_p imply phosphorus release rates from the sediment within the range of 1.2–1.6 mg m⁻² day⁻¹, suggesting that the internal loading can conceivably be another factor to influence the duration of the transient phase and the recovery resilience of the Harbour (Jeppesen et al., 2005; Dittrich et al., 2009). Yet, there is a surprising absence of studies to have rigorously quantified the release of phosphorus from the sediments of the Harbour, while the relevant fluxes have been historically assumed minimal (Mayer and Manning, 1990). In this context, if we also consider that the hypoxia in the Harbour waters will continue to be an issue (HHTT-WQ, 2007), we believe that the discrepancy between our predictions and the lower estimates reported from other empirical (or modeling) studies invites further examination of the likelihood that the internal loading may exert control on the summer hypolimnetic phosphorus accumulation (>25 µg TP L⁻¹).

In conclusion, we presented a Bayesian modeling framework that evaluates the outcome of alternative management scenarios (i.e., critical nutrient loads) based on acceptable confidence of compliance levels with different water quality criteria in Hamilton Harbour. Our analysis suggests that the water quality goal for TP (17 µg L⁻¹) will likely be met with a reasonably low violation frequency (<15%), if the recommendation for phosphorus loading at the level of 142 kg day⁻¹ is accomplished. Yet, the attainment of the water quality goal related to the summer chlorophyll *a* concentrations has not been clearly demonstrated, and the central tendency of our predictions indicates a marginal exceedance of the 10 µg L⁻¹ threshold value, even when the exogenous TP loading complies with the most extreme reduction propositions. Our study also provides evidence that the anticipated structural shifts of the zooplankton community will determine the restoration rate of the Harbour, while two critical aspects of the food web dynamics will likely modulate the stability of the new trophic state, i.e., the coupling between the benthic and pelagic habitat and the relative importance of the allochthonous organic matter in sustaining the secondary production in the system. We also argue that the bottom-up approach historically followed in the Harbour was sufficient to bring the system in its present state, but any further improvements should be viewed in the context of a combined bottom-up and top-down control. Finally, we emphasize that our results are conditional upon the assumptions

made regarding the contemporary nutrient loading estimates along with what was perceived as present water quality conditions in the Harbour. Future work should revisit some of these assumptions and further examine the robustness of the projected trajectories of the major cause-effect relationships pertaining to water quality management.

A little more than three decades ago, Vollenweider (1976) stated that “If further progress should be possible, then more complex models are needed. It seems to be particularly important to obtain a better hold on parameters which also exert an influence on loading tolerance, such as length of stratification, mixing cycles, depth of thermocline, hypolimnetic entrainment, water discharge and loading cycles, etc. Also, the trophic-dynamic interrelationships in the sense of Lindeman (1942) require much more sophisticated analyses.” While Vollenweider’s plea still reflects one of the challenges of the current modeling practice, we believe that equally important are the development of techniques that rigorously assess the reliability of the critical planning information generated by the models. This statement should not be viewed as an excuse to hide behind the model uncertainty but rather an attempt to differentiate the predictable from the unpredictable patterns and critically evaluate the model outputs. Modeling is a complementary tool that should be part of any adaptive management implementation effort. It can verify the plausibility of hypotheses, identify unanticipated system responses, generate research questions, and provide predictions conditional on the assumptions made. If the assumptions are incorrect or uncertain, then our task is to revisit them to further improve our projections.

Acknowledgments

This project has received funding support from the Ontario Ministry of the Environment (Canada-Ontario Grant Agreement 120808). Such support does not indicate endorsement by the Ministry of the contents of this material. Maryam Ramin has received support from the Natural Sciences and Engineering Research Council of Canada (Doctoral Scholarships). All the material pertinent to this analysis is available upon request from the corresponding author.

Appendix. Supplementary information

Supplementary information associated with this article can be found, in the online version, at doi.10.1016/j.envsoft.2010.08.006.

References

- Arhonditsis, G.B., Tsirois, G., Karydis, M., 2002. The effects of episodic rainfall events to the dynamics of coastal marine ecosystems: applications to a semi-enclosed gulf in the Mediterranean Sea. *J. Mar. Syst.* 35, 183–205.
- Arhonditsis, G.B., Brett, M.T., 2004. Evaluation of the current state of mechanistic aquatic biogeochemical modeling. *Mar. Ecol. Prog. Ser.* 271, 13–26.
- Arhonditsis, G.B., Brett, M.T., De Gasperi, C.L., Schindler, D.E., 2004. Effects of climatic variability on the thermal properties of Lake Washington. *Limnol. Oceanogr.* 49, 256–270.
- Arhonditsis, G.B., Brett, M.T., 2005. Eutrophication model for Lake Washington (USA). Part I. Model description and sensitivity analysis. *Ecol. Modell.* 187, 140–178.
- Arhonditsis, G.B., Adams-VanHarn, B.A., Nielsen, L., Stow, C.A., Reckhow, K.H., 2006. Evaluation of the current state of mechanistic aquatic biogeochemical modeling: citation analysis and future perspectives. *Environ. Sci. Technol.* 40, 6547–6554.
- Arhonditsis, G.B., Qian, S.S., Stow, C.A., Lamon, E.C., Reckhow, K.H., 2007. Eutrophication risk assessment using Bayesian calibration of process-based models: application to a mesotrophic lake. *Ecol. Modell.* 208, 215–229.
- Arhonditsis, G.B., Papantou, D., Zhang, W.T., Perhar, G., Massos, E., Shi, M.L., 2008a. Bayesian calibration of mechanistic aquatic biogeochemical models and benefits for environmental management. *J. Mar. Syst.* 73, 8–30.

- Arhonditsis, G.B., Perhar, G., Zhang, W.T., Massos, E., Shi, M., Das, A., 2008b. Addressing equifinality and uncertainty in eutrophication models. *Water Resour. Res.* 44, W01420.
- Barica, J., 1989. Unique limnological phenomena affecting water quality of Hamilton Harbour, Lake Ontario. *J. Great Lakes Res.* 15, 519–530.
- Barnett, V., O'Hagan, A., 1997. *Setting Environmental Standards: The Statistical Approach to Handling Uncertainty and Variation*. Chapman & Hall, London.
- Bastviken, D.T.E., Caraco, N.F., Cole, J.J., 1998. Experimental measurements of zebra mussel (*Dreissena polymorpha*) impacts on phytoplankton community composition. *Freshw. Biol.* 39, 375–386.
- Bierman, V.J., Kaur, J., DePinto, J.V., Feist, T.J., Dilks, D.W., 2005. Modeling the role of zebra mussels in the proliferation of blue-green algae in Saginaw Bay, Lake Huron. *J. Great Lakes Res.* 31 (1), 32–55.
- Borsuk, M.E., Stow, C.A., Reckhow, K.H., 2002. Predicting the frequency of water quality standard violations: a probabilistic approach for TMDL development. *Environ. Sci. Technol.* 36, 2109–2115.
- Brett, M.T., Kainz, M.J., Taipale, S.J., Seshan, H., 2009. Phytoplankton, not allochthonous carbon, sustains herbivorous zooplankton production. *Proc. Natl. Acad. Sci. U.S.A.* 106, 21197–21201.
- Budd, J.W., Drummer, T.D., Nalepa, T.F., Fahnenstiel, G.L., 2001. Remote sensing of biotic effects: zebra mussels (*Dreissena polymorpha*) influence on water clarity in Saginaw Bay, Lake Huron. *Limnol. Oceanogr.* 46, 213–223.
- Burley, M., 2007. Water quality and phytoplankton photosynthesis. *Can. Tech. Rep. Fish. Aquat. Sci.* 2729, 9–42.
- Canale, R.P., Chapra, S.C., 2002. Modeling zebra mussel impacts on water quality of Seneca River, New York. *J. Environ. Eng.* 128, 1158–1168.
- Cerco, C.F., Cole, T.M., 1994. CE-QUAL-ICM: A Three-Dimensional Eutrophication Model, Version 1.0. User's Guide. US Army Corps of Engineers Waterways Experiments Station, Vicksburg, MS.
- Chapra, S.C., Dobson, H.F.H., 1981. Quantification of the lake trophic typologies of Naumann (surface quality) and Thienemann (oxygen) with special reference to the Great Lakes. *J. Great Lakes Res.* 7, 182–193.
- Charlton, M.N., 2001. The Hamilton Harbour remedial action plan: eutrophication. *Verh. Internat. Verein. Limnol.* 27, 4069–4072.
- Chow-Fraser, P., Loughheed, V.L., Crosbie, B., LeThiec, V., Simser, L., Lord, J., 1998. Long-term response of the biotic community to fluctuating water levels and changes in water quality in Cootes Paradise Marsh, a degraded coastal wetland of L. Ontario. *Wetland Ecol. Manage.* 6, 19–42.
- Clark, J.S., Carpenter, S.R., Barber, M., Collins, S., Dobson, A., Foley, J.A., Lodge, D.M., Pascual, M., Pielke, R., Pizer, W., Pringle, C., Reid, W.V., Rose, K.A., Sala, O., Schlesinger, W.H., Wall, D.H., Wear, D., 2001. Ecological forecasts: an emerging imperative. *Science* 293, 657–660.
- Dennis, B., 1996. Discussion: should ecologists become Bayesians? *Ecol. Appl.* 6, 1095–1103.
- Dermott, R., Bonnell, R., 2007. Benthic fauna in Hamilton Harbour: 2002–2003. *Can. Tech. Rep. Fish. Aquat. Sci.* 2729, 91–120.
- Dermott, R., Johannsson, O., Munawar, M., Bonnell, R., Bowen, K., Burley, M., Fitzpatrick, M., Gerlofsma, J., Niblock, H., 2007. Assessment of lower food web in Hamilton Harbour, Lake Ontario, 2002–2004. *Can. Tech. Rep. Fish. Aquat. Sci.* 2729, 120.
- Dillon, P.J., Rigler, F.H., 1974. Phosphorus–chlorophyll relationship in lakes. *Limnol. Oceanogr.* 19, 767–773.
- Dittrich, M., Wehrli, B., Reichert, P., 2009. Lake sediments during the transient eutrophication period: reactive-transport model and identifiability study. *Ecol. Modell.* 220, 2751–2769.
- Downing, J.A., Rigler, F.H., 1984. *A Manual on Methods for the Assessment of Second Productivity in Fresh Water*, second ed. Blackwell Scientific Publications, Oxford, UK.
- Edmondson, W.T., 1994. Sixty years of Lake Washington: a curriculum vitae. *Lake Reserv. Manage.* 10, 75–84.
- Edwards, A.M., Yool, A., 2000. The role of higher predation in plankton population models. *J. Plankton Res.* 22, 1085–1112.
- Effler, S.W., Boone, S.R., Siegrid, C.A., Walrath, L., Ashby, S.L., 1997. Mobilization of ammonia and phosphorus by zebra mussels (*Dreissena polymorpha*) in the Seneca River, New York. In: D'Itri, F.M. (Ed.), *Zebra Mussels and Aquatic Nuisance Species*. CRC Press LLC, Boca Raton, FL, pp. 187–207.
- Ellison, A.M., 2004. Bayesian inference in ecology. *Ecol. Lett.* 7, 509–520.
- Eppley, R.W., Peterson, B.J., 1979. Particulate organic-matter flux and planktonic new production in the deep ocean. *Nature* 282, 677–680.
- Fahnenstiel, G.L., Lang, G.A., Nalepa, T.F., Johengen, T.H., 1995. Effects of zebra mussel (*Dreissena polymorpha*) colonization on water quality parameters in Saginaw Bay, Lake Huron. *J. Great Lakes Res.* 21, 435–448.
- Fasham, M.J.R., Ducklow, H.W., McKelvie, S.M., 1990. A nitrogen based model of plankton dynamics in the oceanic mixed layer. *J. Mar. Res.* 48, 591–639.
- Gelman, A., Carlin, J.B., Stern, H.S., Rubin, D.B., 1995. *Bayesian Data Analysis*. Chapman and Hall, New York.
- Gerlofsma, J., Bowen, K., Johannsson, O., 2007. Zooplankton in Hamilton Harbour 2002–2004. *Can. Tech. Rep. Fish. Aquat. Sci.* 2729, 65–90.
- Gilks, W.R., Richardson, S., Spiegelhalter, D.J., 1998. *Markov Chain Monte Carlo in Practice*. Chapman & Hall/CRC, pp. 512.
- Gudimov, A., Ramin, M., Stremilov, S., Arhonditsis, G.B., 2010. Eutrophication risk assessment in Hamilton Harbour: system analysis and evaluation of nutrient loading scenarios. *J. Great Lakes Res.* 36, 520–539.
- Hall, J.D., O'Connor, K., Ranieri, J., 2006. Progress toward delisting a Great Lakes area of concern: the role of integrated research and monitoring in the Hamilton Harbour remedial action plan. *Environ. Monit. Assess.* 113, 227–243.
- Hamblin, P.F., He, C., 2003. Numerical models of the exchange flows between Hamilton Harbour and Lake Ontario. *Can. J. Civ. Eng.* 30, 168–180.
- Hamilton Harbour RAP Technical Team, 2004. 1996–2002 Contaminant Loadings and Concentrations to Hamilton Harbour. Hamilton Harbour Technical Team–Water Quality 2007.
- Hamilton Harbour Technical Team–Water Quality, 2007. Hamilton Harbour RAP Water Quality Goals and Targets Review, Part 1: Response to the City of Hamilton's Proposed Wastewater System Upgrades (Technical appendix).
- Hamilton, D.P., Schladow, S.G., 1997. Prediction of water quality in lakes and reservoirs. Part 1. Model description. *Ecol. Modell.* 96, 91–110.
- Hiriart-Baer, V.P., Milne, J., Charlton, M.N., 2009. Water quality trends in Hamilton Harbour: two decades of change in nutrients and chlorophyll *a*. *J. Great Lakes Res.* 35, 293–301.
- James, W.F., Barko, J.W., Eakin, H.L., 1997. Nutrient regeneration by the zebra mussel (*Dreissena polymorpha*). *J. Freshw. Ecol.* 12, 209–216.
- Jassby, A.D., Platt, T., 1976. Mathematical formulation of relationship between photosynthesis and light for phytoplankton. *Limnol. Oceanogr.* 21, 540–547.
- Jeppesen, E., Sondergaard, M., Jensen, J.P., Havens, K.E., Anneville, O., Carvalho, L., Coveney, M.F., Deneke, R., Dokulil, M.T., Foy, B., Gerdeaux, D., Hampton, S.E., Hilt, S., Kangur, K., Kohler, J., Lammens, E.H.H.R., Lauridsen, T.L., Manca, R., Miracle, M.R., Moss, B., Noges, P., Persson, G., Phillips, G., Portielje, R., Schelske, C.L., Straile, D., Tatrai, I., Willen, E., Winder, M., 2005. Lake responses to reduced nutrient loading: an analysis of contemporary long-term data from 35 case studies. *Freshw. Biol.* 50, 1747–1771.
- Johannsson, O.E., Dermott, R., Graham, D.M., Dahl, J.A., Millard, E.S., Myles, D.D., LeBlanc, J., 2000. Benthic and pelagic secondary production in Lake Erie after the invasion of *Dreissena* spp. with implications for fish production. *J. Great Lakes Res.* 26, 31–54.
- Klapwijk, A., Snodgrass, W.J., 1985. Model for lake–bay exchange flow. *J. Great Lakes Res.* 11, 43–52.
- Lindeman, R.L., 1942. Seasonal food cycle dynamics in a senescent lake. *Am. Midl. Nat.* 26, 636–726.
- Maclsaac, H.J., Sprules, W.G., Johannsson, O.E., Leach, J.H., 1992. Filtering impacts of larval and sessile zebra mussels (*Dreissena polymorpha*) in Western Lake Erie. *Oecologia* 92, 30–39.
- Makarewicz, J.C., Lewis, T.W., Bertram, P., 1999. Phytoplankton composition and biomass in the offshore waters of Lake Erie: pre- and post-*Dreissena* introduction (1983–1993). *J. Great Lakes Res.* 25, 135–148.
- Marvin, C.H., McCarry, B.E., Villella, J., Allan, L.M., Bryant, D.W., 2000. Chemical and biological profiles of sediments as indicators of sources of contamination in Hamilton Harbour. Part II: bioassay-directed fractionation using the Ames Salmonella/microsome assay. *Chemosphere* 41, 989–999.
- Mazumder, A., 1994. Patterns of algal biomass in dominant odd-link vs even-link lake ecosystems. *Ecology* 75 (4), 1141–1149.
- Mayer, T., Manning, P.G., 1990. Inorganic contaminants in suspended solids from Hamilton Harbour. *J. Great Lakes Res.* 16, 299–318.
- Mills, E.L., Green, D.M., Schiavone Jr., A., 1987. Use of zooplankton size to assess the community structure of fish populations in freshwater lakes. *N. Am. J. Fish. Manage.* 7, 369–378.
- Millard, E.S., Sager, P.E., 1994. Comparison of phosphorus, light, climate, and photosynthesis between 2 culturally eutrophied bays – Green Bay, Lake Michigan, and the Bay of Quinte, Lake Ontario. *Can. J. Fish. Aquat. Sci.* 51, 2579–2590.
- Munawar, M., and Fitzpatrick, M., 2007. An integrated assessment of the microbial and planktonic communities of Hamilton Harbour. In: R. Dermott, O. Johannsson, M. Munawar, R. Bonnell, K. Bowen, M. Burley, M. Fitzpatrick, J. Gerlofsma, and H. Niblock. *Assessment of Lower Food Web in Hamilton Harbour, Lake Ontario, 2002–2004*. *Can. Tech. Rep. Fish. Aquat. Sci.* vol. 2729: 43–63.
- Munawar, M., Dermott, R., McCarthy, L.H., Munawar, S.F., van Stam, H.A., 1999. A comparative bioassessment of sediment toxicology in lentic and lotic ecosystems of the North American Great Lakes. *Aquat. Ecosyst. Health* 2, 367–378.
- Nicholls, K.H., Heintsch, L., Carney, E., 2002. Univariate step-trend and multivariate assessments of the apparent effects of P loading reductions and zebra mussels on the phytoplankton of the Bay of Quinte, Lake Ontario. *J. Great Lakes Res.* 28, 15–31.
- Office of Water, 1997. *Guidelines for Preparation of the Comprehensive State Water Quality Assessments*. U.S. Washington, DC: Environmental Protection Agency.
- Pace, M.L., 2001. Prediction and the aquatic sciences. *Can. J. Fish. Aquat. Sci.* 58, 63–72.
- Reckhow, K.H., Arhonditsis, G.B., Kenney, M.A., Hauser, L., Tribo, J., Wu, C., Elcock, K.J., Steinberg, L.J., Stow, C.A., McBride, S.J., 2005. A predictive approach to nutrient criteria. *Environ. Sci. Technol.* 39, 2913–2919.
- Rukavina, N.A., Versteeg, J.K., 1996. Surficial sediments of Hamilton Harbour: physical properties and basin morphology. *Wat. Qual. Res. J. Can.* 31, 529–551.
- Scheffer, M., van Nes, E.H., 2004. Mechanisms for marine regime shifts: can we use lakes as microcosms for oceans? *Prog. Oceanogr.* 60, 303–319.
- Smith, T., Stevenson, R., Caraco, N., Cole, J., 1998. Changes in phytoplankton community structure during the zebra mussel (*Dreissena polymorpha*) invasion of the Hudson River (New York). *J. Plank. Res.* 20, 1567–1579.
- Steinberg, L.J., Reckhow, K.H., Wolpert, R.L., 1997. Characterization of parameters in mechanistic models: a case study of a PCB fate and transport model. *Ecol. Modell.* 97, 35–46.

- Stow, C.A., Larnon, E.C., Qian, S.S., Soranno, P.A., Reckhow, K.H., 2009. Bayesian Hierarchical/Multilevel Models for Inference and Prediction Using Cross-System Lake Data. Springer.
- Tian, R.C., Vezina, A.F., Starr, M., Saucier, F., 2001. Seasonal dynamics of coastal ecosystems and export production at high latitudes: a modeling study. *Limnol. Oceanogr.* 46, 1845–1859.
- Vanderploeg, H.A., Liebig, J.R., Carmichael, W.W., Agy, M.A., Johengen, T.H., Fahnenstiel, G.L., Nalepa, T.F., 2001. Zebra mussel (*Dreissena polymorpha*) selective filtration promoted toxic microcystis blooms in Saginaw Bay (Lake Huron) and Lake Erie. *Can. J. Fish. Aquat. Sci.* 58, 1208–1221.
- Van Oijen, M., Rougier, J., Smith, R., 2005. Bayesian calibration of process-based forest models: bridging the gap between models and data. *Tree Physiol.* 25, 915–927.
- Vollenweider, R.A., 1976. Advances in defining critical loading levels for phosphorus in lake eutrophication. *Mem. 1st. Ital. Idrobiol.* 33, 53–83.
- Wroblewski, J.S., 1977. Model of phytoplankton plume formation during variable Oregon upwelling. *J. Mar. Res.* 35, 357–394.
- Zhang, W., Arhonditsis, G.B., 2008. Predicting the frequency of water quality standard violations using Bayesian calibration of eutrophication models. *J. Great Lakes Res.* 34, 698–720.
- Zhang, W., Arhonditsis, G.B., 2009. A Bayesian hierarchical framework for calibrating aquatic biogeochemical models. *Ecol. Modell.* 220, 2142–2161.

**INTEGRATION OF MATHEMATICAL MODELING AND BAYESIAN
INFERENCE FOR SETTING WATER QUALITY CRITERIA IN HAMILTON
HARBOUR, ONTARIO, CANADA**

(Electronic Supplementary Material)

**Maryam Ramin¹, Serguei Stremilov¹, Tanya Labencki², Alexey Gudimov¹, Duncan Boyd², and
George B. Arhonditsis^{1*}**

¹Ecological Modeling Laboratory,
Department of Physical & Environmental Sciences, University of Toronto,
Toronto, Ontario, Canada, M1C 1A4

²Water Monitoring & Reporting Section, Environmental Monitoring and Reporting Branch,
Ontario Ministry of the Environment, Toronto, Ontario, Canada, M9P 3V6

* Corresponding author

e-mail: georgea@utsc.utoronto.ca, Tel.: +1 416 208 4858; Fax: +1 416 287 7279.

Numerical approximations for posterior distributions

Following the methodological protocol presented in several recent studies (Arhonditsis et al., 2007; 2008a,b; Zhang and Arhonditsis, 2008), sequence of realizations from the posterior distribution of the model were obtained using Markov chain Monte Carlo (MCMC) simulations (Gilks et al., 1998). We used the general normal-proposal Metropolis algorithm coupled with an ordered over-relaxation to control the serial correlation of the MCMC samples (Neal, 1998). In this study, we are testing two parallel chains with starting points: (i) a vector that consists of the mean values of the prior parameter distributions, and (ii) a vector based on a preliminary calibration of the model. The model was run for 40,000 iterations and convergence was assessed with the modified Gelman–Rubin convergence statistic (Brooks and Gelman, 1998). The accuracy of the posterior estimates was inspected by assuring that the Monte Carlo error (an estimate of the difference between the mean of the sampled values and the true posterior mean; see Spiegelhalter et al., 2003) for all the parameters is less than 5% of the sample standard deviation. Our framework is implemented in the WinBUGS Differential Interface (WBDiff); an interface that allows numerical solution of systems of ordinary differential equations within the WinBUGS software.

References

- Arhonditsis, G.B., Qian, S.S., Stow, C.A., Lamon, E.C., and Reckhow, K.H. 2007. Eutrophication risk assessment using Bayesian calibration of process-based models: Application to a mesotrophic lake. *Ecol. Model.* **208**: 215-229.
- Arhonditsis, G.B., Papantou, D., Zhang, W.T., Perhar, G., Massos, E., and Shi, M.L. 2008a. Bayesian calibration of mechanistic aquatic biogeochemical models and benefits for environmental management. *J. Mar. Syst.* **73**: 8-30.
- Arhonditsis, G.B., Perhar, G., Zhang, W.T., Massos, E., Shi, M., and Das, A. 2008b. Addressing equifinality and uncertainty in eutrophication models. *Water Resour. Res.* **44**: W01420.

- Brooks, S.P., and Gelman, A. 1998. Alternative methods for monitoring convergence of iterative simulations. *J. Comput. Graph. Stat.* **7**: 434-455.
- Gilks, W.R., Richardson, S., and Spiegelhalter, D.J. 1998. Markov Chain Monte Carlo in Practice. Chapman & Hall/CRC, 512 p.
- Neal, R. 1998. Suppressing random walks in Markov chain Monte Carlo using ordered over-relaxation. In: Jordan, M.I. (Ed.) *Learning in Graphical Models*. pp. 205-230. Dordrecht: Kluwer Academic Publishers.
- Spiegelhalter, D. J., Thomas, A., Best, N. G. and Lunn, D. 2003. WinBUGS User Manual (Version 1.4). Cambridge: Mrc Biostatistics Unit, www.mrc-bsu.cam.ac.uk/bugs/.
- Zhang, W., and Arhonditsis, G.B. 2008. Predicting the frequency of water quality standard violations using Bayesian calibration of eutrophication models. *J. Great Lakes Res.* **34**: 698-720.

Table 1-ESM: Mathematical description of the model. The i and x indices refer to the *phytoplankton*, *cyanobacteria* and *epilimnion*, *hypolimnion*, respectively.

No.	State Variable	Term	Equation
1	Phytoplankton biomass	$\frac{dPHYT_{i,x}}{dt}$	$= growth_{i,x} \times PHYT_{i,x} - mp_i \times e^{kt(T_x - Tempref)} \times PHYT_{i,x} - Vsettlng_i \times PHYT_{i,x} / z_x - filter_i \times e^{k_{filt}(T_x - Tempref)} \times PHYT_{i,x} - Grazing_{i,x} \times ftemperature_x \times ZOO P_x \pm Exchanges_{PHYT i Vertical} \pm Exchanges_{PHYT i Lake Ontario}$
	Growth rate	$growth_{i,x}$	$= growthmax_i \times fnutrient_{i,x} \times flight_{i,x} \times ftemperature_{i,x}$
	Nutrient limitation	$fnutrient_{i,x}$	$= \min\{\phi NA_{i,x}, \phi PO4_{i,x}\}$
	Nitrogen limitation	$\phi NA_{i,x}$	$= \phi NO3_{i,x} + \phi NH4_{i,x}$
	Nitrate limitation	$\phi NO3_{i,x}$	$= (NO3_x e^{-\psi NH4_x}) / (NO3_x + NH_i)$
	Ammonium limitation	$\phi NH4_{i,x}$	$= NH4_x / (NH4_x + AH_i)$
	Phosphate limitation	$\phi PO4_{i,x}$	$= (Pint_{i,x} - Pmin_i) / (Pmax_i - Pmin_i)$
	Intracellular phosphorus content	$\frac{dPint_{i,x}}{dt}$	$= Pup_{i,x} \times Pfb_{i,x} - growth_{i,x} \times Pint_{i,x}$, where
	Phosphorus uptake	$Pup_{i,x}$	$= Pmaxuptake_i \times (PO4_x / (PO4_x + PH_i))$
	Feedback control	$Pfb_{i,x}$	$= (Pmax_i - Pint_{i,x}) / (Pmax_i - Pmin_i)$
	Light limitation	$flight_{i,x}$	$= 2.718 \times (FD / (kext_x \times z_x)) (e^{-a1} - e^{-a0})$; where $a0_i = (I/k_i) e^{-kext_x \times H_x}$, $a1_i = (I/k_i) e^{-kext_x(z_x + H_x)}$
Light attenuation	$kext_x$	$= kchla_i \sum_i PHYT_{i,x} \times ChlaC_i + kbackground$	
Temperature limitation	$ftemperature_{i,x}$	$= \exp(-KTgr_i(T_x - Topt_i^2))$	
		FD	$= \text{the fractional day length } (0 \leq FD \leq 1)$
2	Zooplankton biomass	$\frac{dZOO P_x}{dt}$	$= [\sum_i Grazing_{i,x} \times ftemperature_x \times asfood_i + Grazing_{det,x} \times ftemperature_x \times asfood_{det}] \times ZOO P_x - mz \times e^{kt(T_x - Tempref)} \times ZOO P_x \pm Exchanges_{ZOO P Vertical} \pm Exchanges_{ZOO P Lake Ontario}$
	Grazing rate for phytoplankton	$Grazing_{i,x}$	$= maxgrazing \times (Pref_{i,x} \times PHYT_{i,x}) / (KZ + Food_x)$
	Grazing rate for detritus	$Grazing_{det,x}$	$= maxgrazing \times (Pref_{det,x} \times Detritus_x) / (KZ + Food_x)$
	Abundance of food in layer x	$Food_x$	$= \sum_i Pref_{i,x} \times PHYT_{i,x} + Pref_{det,x} \times Detritus_x$
	Preference of zooplankton for phytoplankton i	$Pref_{i,x}$	$= (Pref_i \times PHYT_{i,x}) / (\sum_i Pref_i \times PHYT_{i,x} + Pref_{det} \times Detritus_x)$
	Preference of zooplankton for detritus	$Pref_{det,x}$	$= (Pref_{det} \times Detritus_x) / (\sum_i Pref_i \times PHYT_{i,x} + Pref_{det} \times Detritus_x)$
Temperature limitation for	$ftemperature_x$	$= \exp(-KTgr_{zoop}(T_x - Topt)^2)$	

No.	State Variable	Term	Equation
	growth		
3	Detritus concentration	$\frac{dDetritus_x}{dt}$	$= \sum_i [(1 - \alpha_{DOCi}) \times mp_i \times e^{kt(T_x - Tempref)} \times PHYT_{i,x}] + [(1 - \alpha_{DOC_{zoop}}) \times mz \times e^{kt(T_x - Tempref)} \times ZOOP_x] - [(maxgrazing \times Pref_{det,x} \times Detritus_x) / (KZ + Food_x)] \times ftemperature_x \times ZOOP_x - Vsettlng_{(biogenic)} \times Detritus_x / z_x - KCmineral_x \times Detritus_x$
	Carbon mineralization rate	$KCmineral_x$	$= ftemperature_min_x \times KCrefmineral$; where
	Temperature limitation for mineralization	$ftemperature_min_x$	$= exp(-KTFmin \times (T_x - Toptmin)^2)$
4	Phosphate concentration	$\frac{dPO_{4x}}{dt}$	$= - \sum_i P_{up_{i,x}} \times P_{fb_{i,x}} \times PHYT_{i,x} + \sum_i \alpha_{PO4i} \times mp_i \times e^{kt(T_x - Tempref)} \times Pint_{i,x} \times PHYT_{i,x} + \alpha_{PO4_{zoop}} \times mz \times e^{kt(T_x - Tempref)} \times P/C_{zoop} \times ZOOP_x + KPmineral_x \times OP_x - FePrecipitation \pm ExchangesPO_{4Vertical} \pm ExchangesPO_{4Lake Ontario} + PO_{4EXOG_{EPI}} + PO_{4ENDOG_x}$, where
	Phosphorus mineralization rate	$KPmineral_x$	$= ftemperature_min_x \times KPrefmineral$; where
	Iron-induced precipitation due to Steel Mills discharge	$FePrecipitation$	$= (1 - (9.4 \times [Fe_{Steel Mills} + 1400]^{-0.31})) \times PO_{4x}$
5	Organic phosphorus concentration	$\frac{dOP_x}{dt}$	$= DetritusP_x - DetritusGrazingP_x \times ftemperature_x \times ZOOP_x - SettlingP_x \times OP_x / z_x - KPmineral_x \times OP_x \pm ExchangesOP_{Vertical} \pm ExchangesOP_{Lake Ontario} + OPEXOG_{EPI} + OPENDOG_x$
	Biogenic organic phosphorus accumulation	$DetritusP_x$	$= \sum_i (1 - \alpha_{PO4i}) \times mp_i \times e^{kt(T_x - Tempref)} \times Pint_{i,x} \times PHYT_{i,x} + (1 - \alpha_{PO4_{zoop}}) \times mz \times e^{kt(T_x - Tempref)} \times P/C_{zoop} \times ZOOP_x$
	Loss due to zooplankton grazing upon detritus	$DetritusGrazingP_x$	$= (maxgrazing \times Pref_{det,x} \times DetritusP_x) / (KZ + Food_x)$
	Loss due to particulate phosphorus settling	$SettlingP_x$	$= (DetritusP_x / OP_x) \times Vsettlng_{(biogenic)} + (1 - (DetritusP_x / OP_x)) \times Vsettlng$
6	Ammonium concentration	$\frac{dNH_{4x}}{dt}$	$= - \sum_i \varphi_{NH4_{i,x}} \times growthmax_i \times flight_{i,x} \times ftemperature_{i,x} \times N/C_{i,x} \times PHYT_{i,x} + \sum_i \alpha_{NH4_i} \times mp_i \times e^{kt(T_x - Tempref)} \times N/C_{i,x} \times PHYT_{i,x} + \alpha_{NH4_{zoop}} \times mz \times e^{kt(T_x - Tempref)} \times N/C_{zoop} \times ZOOP_x + KNmineral_x \times ON_x - Nitrification_x \pm ExchangesNH4_{Vertical} \pm ExchangesNH4_{Lake Ontario} + NH4EXOG_{EPI} + NH4ENDOG_x$
	Mineralization rate	$KNmineral_x$	$= KNrefmineral \times ftemperature_min_x$
	Nitrification rate	$Nitrification_x$	$= Nitrifmax \times flightnitr_x \times (DO_x / (DO_x + KHdonit)) \times (NH4_x / KHnh4nit + NH4_x) \times ftempnitr_x$
	Light limitation	$flightnitr_x$	$= 1$ when $I_x \leq 0.1 \times I$, else $flightnitr_x = 0$
	Temperature limitation	$ftempnitr_x$	$= exp(-KTgrnitr(T_x - Toptnitr)^2)$
	Intensity of light in	I_x	$= I / (kext_x \times z_x) (e^{-kext_x \times Hx} - e^{-kext_x(z_x + Hx)})$

No.	State Variable	Term	Equation
	compartments x		
	Nitrogen-to-carbon ratio of the phytoplankton cells	$N/C_{i,x}$	$= 16 \times Pint_{i,x}$
7	Nitrate concentration	$\frac{dNO_{3x}}{dt}$	$= - \sum_i \varphi NO_{3i,x} \times growthmax_i \times flight_{i,x} \times ftemperature_{i,x} \times N/C_{i,x}$ $\times PHYT_{i,x} + Nitrification_x - Denitrification_x \pm ExchangesNO3_{Vertical}$ $\pm ExchangesNO3_{LakeOntario} + NO3EXOG_{EPI} + NO3ENDOG_x$
	Denitrification rate	$Denitrification_x$	$= Denitrifmax \times (KHdodenit / (DO_x + KHdodenit))$ $\times (NO_{3x} / KHno3nit + NO_{3x}) \times ftempdenitr_x$
	Temperature limitation	$ftempdenitr_x$	$= \exp(-KTgrdenitr(T_x - Toptdenitr)^2)$
8	Organic nitrogen concentration	$\frac{dON_x}{dt}$	$= Detritus N_x - DetritusGrazing N_x \times ftemperature_x \times ZOOP_x$ $- [Detritus N_x / ON_x \times Vsettlng_{(biogenic)} + (1 - Detritus N_x / ON_x)$ $\times Vsettlng] \times ON_x / z_x - KNmineral_x \times ON_x \pm ExchangesON_{Vertical}$ $\pm ExchangesON_{LakeOntario} + ONEXOG_{EPI} + ONENDOG_x$
	Biogenic organic nitrogen accumulation	$Detritus N_x$	$= \sum_i (1 - aNH4_i) \times mp_i \times e^{kt(T_x - Tempref)} \times N/C_{i,x} \times PHYT_{i,x}$ $+ (1 - aNH4_{zoop}) \times mz \times e^{kt(T_x - Tempref)} \times N/C_{zoop} \times ZOOP_x$
	Loss due to zooplankton grazing upon detritus	$DetritusGrazingN_x$	$= maxgrazing \times Pref_{det,x} \times Detritus N_x / (KZ + Food_x)$
9	Sediment submodel		
9.1	Phosphate sediment release	$\frac{dPO_{4sed,x}}{dt}$	$= (1 - \beta_p) \times Pdeposition - (as_{PO4} \times PO_{4sed,x} \times e^{ktsed(Tsedx - Temprefsed)})$
	Organic phosphorus sedimentation	$Pdeposition$	$= \left(\sum_i Vsettlng_i \times Pint_{i,x} \times PHYT_{i,x} + SettlingP_x \times OP_x \right)$
9.2	Ammonium sediment release	$\frac{dNH_{4sed,x}}{dt}$	$= (1 - \beta_N) \times Ndeposition - (as_{NH4} \times NH_{4sed,x} \times e^{ktsed(Tsedx - Temprefsed)})$ $- Nitrifmax_{sed} \times (DO_x / (DO_x + KHdonit_{sed}))$ $\times (NH_{4sed,x} / (KHnh4nit_{sed} + NH_{4sed,x})) \times ftempnitr_{sed,x}$
	Loss due to particulate nitrogen settling	$Ndeposition$	$= \sum_i Vsettlng_i \times N/C_{i,x} \times PHYT_{i,x} + VsettlngN_x \times ON_x$
	Temperature limitation for nitrification in the sediments	$ftempnitr_{sed,x}$	$= \exp(-KTgrnitr_{sed}(T_x - Toptnitr_{sed})^2)$
9.3	Nitrate sediment release	$\frac{dNO_{3sed,x}}{dt}$	$= Nitrifmax_{sed} \times (DO_x / (DO_x + KHdonit)) \times (NH_{4sed,x} / (KHnh4nit + NH_{4sed,x}))$ $\times ftempnitr_x - (as_{NO3} \times NO_{3sed,x} \times e^{ktsed(Tsedx - Temprefsed)})$ $- Denitrifmax_{sed} \times (KHdodenit_{sed} / (DO_x + KHdodenit_{sed}))$ $\times (NO_{3sed,x} / (KHno3denit_{sed} + NO_{3sed,x})) \times ftempdenitr_{sed,x}$
	Temperature limitation for denitrification in the sediments	$ftempdenitr_{sed,x}$	$= \exp(-KTgrdenitr_{sed}(T_x - Toptdenitr_{sed})^2)$

No.	State Variable	Term	Equation
	Rate of sediment release of organic nitrogen	$ONSED_x$	$= ONosed \times e^{k_{tsed}(T_{sedx} - Temp_{prefsed})}$
	Rate of sediment release of organic phosphorus	$OPSED_x$	$= OPosed \times e^{k_{tsed}(T_{sedx} - Temp_{prefsed})}$
		$OPosed$	$= 0.1 \text{ mg m}^{-2} \text{ day}^{-1}$
		$ONosed$	$= OPosed \times TN/TP$
	Total nitrogen to total phosphorus ratio	TN/TP	$= 21$

Table 2-ESM: Description and values of the parameters that were not considered during the Bayesian calibration of the eutrophication model.

<i>Symbol</i>	<i>Description</i>	<i>Values</i>	<i>Units</i>
$\alpha_{DOC\ zoop}$	Fraction of zooplankton mortality becoming dissolved organic carbon	0.5	-
$\alpha_{DOC\ PHYT}$	Fraction of phytoplankton mortality becoming dissolved organic carbon	0.5	-
$\alpha_{DOC\ CY}$	Fraction of cyanobacteria mortality becoming dissolved organic carbon	0.5	-
$\alpha_{NH_4\ zoop}$	Fraction of zooplankton mortality becoming ammonium	0.5	-
$\alpha_{NH_4\ PHYT}$	Fraction of phytoplankton mortality becoming ammonium	0.5	-
$\alpha_{NH_4\ CY}$	Fraction of cyanobacteria mortality becoming ammonium	0.5	-
α_{NO_3}	Sediment nitrate release rate	0.5	day ⁻¹
α_{PO_4}	Sediment phosphate release rate	0.5	day ⁻¹
α_{NH_4}	Sediment ammonium release rate	0.5	day ⁻¹
$\alpha_{PO_4\ zoop}$	Fraction of zooplankton mortality becoming phosphate	0.8	-
$\alpha_{PO_4\ PHYT}$	Fraction of phytoplankton mortality becoming phosphate	0.8	-
$\alpha_{PO_4\ CY}$	Fraction of cyanobacteria mortality becoming phosphate	0.8	-
$\alpha_{food\ det}$	Zooplankton assimilation efficiency for detritus	0.45	-
$\alpha_{food\ PHYT}$	Zooplankton assimilation efficiency for phytoplankton	0.5	-
$\alpha_{food\ CY}$	Zooplankton assimilation efficiency for cyanobacteria	0.15	-
$Chl a C_{PHYT}$	Chlorophyll to carbon ratio in phytoplankton	0.02	-
$Chl a C_{CY}$	Chlorophyll to carbon ratio in cyanobacteria	0.02	-
$Denitrif_{max_{sed}}$	Maximum denitrification rate in the sediments	25	mg N m ⁻² day ⁻¹
$H_{epilimnion}$	Distance from water surface to top of the epilimnion segment layer	0	m
$H_{hypolimnion}$	Distance from water surface to top of the hypolimnion segment	$F(t)$	m
$KH_{dodenit}$	Half saturation concentration of DO deficit required for nitrification	0.5	mg O ₂ m ⁻³
$KH_{dodenit_{sed}}$	Half saturation concentration of DO deficit required for denitrification in the sediments	1	mg O ₂ m ⁻³
KH_{donit}	Half saturation concentration of DO required for nitrification	1	mg O ₂ m ⁻³
$KH_{donit_{sed}}$	Half saturation concentration of DO required for	2	mg O ₂ m ⁻³

<i>Symbol</i>	<i>Description</i>	<i>Values</i>	<i>Units</i>
	nitrification in the sediments		
<i>KHnh4nit</i>	Half saturation concentration of ammonium required for nitrification	1	mg N m ⁻³
<i>KHnh4nit_{sed}</i>	Half saturation concentration of ammonium required for nitrification in the sediments	75	mg N m ⁻³
<i>KHno3denit</i>	Half saturation concentration of nitrate required for denitrification	15	mg N m ⁻³
<i>KHno3denit_{sed}</i>	Half saturation concentration of DO deficit required for denitrification in the sediments	15	mg O ₂ m ⁻³
<i>kt</i>	Effects of temperature on plankton mortality	0.069	°C ⁻¹
<i>ktfilt</i>	Effects of temperature on phytoplankton filtration	0.069	°C ⁻¹
<i>KTFmin</i>	Effects of temperature on mineralization	0.004	°C ⁻²
<i>KTgrdenitr</i>	Effect of temperature on denitrification	0.004	°C ⁻²
<i>KTgrdenitr_{sed}</i>	Effect of temperature on sediment denitrification	0.004	°C ⁻²
<i>KTgr_{zoop}</i>	Effect of temperature on zooplankton	0.005	°C ⁻²
<i>KTgrnitr</i>	Effect of temperature on nitrification	0.004	°C ⁻²
<i>KTgrnitr_{sed}</i>	Effect of temperature on sediment nitrification	0.004	°C ⁻²
<i>KTgr_{PHYT}</i>	Effect of temperature on phytoplankton	0.005	°C ⁻²
<i>KTgr_{CY}</i>	Effect of temperature on cyanobacteria	0.005	°C ⁻²
<i>kt_{sed}</i>	Effects of temperature on sedimentation	0.004	°C ⁻¹
<i>N/C_{zoop}</i>	Nitrogen to carbon ratio for zooplankton	0.2	mg N mg C ⁻¹
<i>Nitrifmax_{sed}</i>	Maximum nitrification rate in the sediments	50	mg N m ⁻² day ⁻¹
<i>P/C_{zoop}</i>	Phosphorus to carbon ratio for zooplankton	0.025	mg P mg C ⁻¹
<i>Pmax_{PHYT}</i>	Maximum phytoplankton internal phosphorus	0.025	mg P mg C ⁻¹
<i>Pmax_{CY}</i>	Maximum cyanobacteria internal phosphorus	0.025	mg P mg C ⁻¹
<i>Pmin_{PHYT}</i>	Minimum phytoplankton internal phosphorus	0.008	mg P mg C ⁻¹
<i>Pmin_{CY}</i>	Minimum cyanobacteria internal phosphorus	0.008	mg P mg C ⁻¹
<i>Pref_{det}</i>	Preference of zooplankton for detritus	1	-
<i>Pref_{PHYT}</i>	Preference of zooplankton for phytoplankton	1.5	-
<i>Pref_{CY}</i>	Preference of zooplankton for cyanobacteria	0.5	-
<i>Tempref</i>	Reference temperature in the water column	20	°C
<i>Tempref_{sed}</i>	Reference temperature in the sediments	20	°C
<i>Toptdenitr</i>	Optimal temperature for denitrification	20	°C
<i>Toptdenitr_{sed}</i>	Optimal temperature for denitrification in the sediments	20	°C
<i>Topt</i>	Reference temperature for zooplankton	20	°C

<i>Symbol</i>	<i>Description</i>	<i>Values</i>	<i>Units</i>
T_{optmin}	Optimal temperature for mineralization	20	°C
$T_{optnitr}$	Optimal temperature for nitrification	20	°C
$T_{optnitr_{sed}}$	Optimal temperature for denitrification in the sediments	20	°C
$T_{opt_{PHYT}}$	Reference temperature for phytoplankton metabolism	20	°C
$T_{opt_{CY}}$	Reference temperature for cyanobacteria metabolism	24	°C
ψ	Strength of the ammonium inhibition for nitrate uptake	0.05	($\mu\text{g N/L}$) ⁻¹
$ExchangesY_{Vertical}$	Diffusive exchanges between the two spatial compartments	$= K_{diffusion} \times \Delta y / \Delta z$ $\times [Epilimnion-Hypolimnion Interface]$	
$ExchangesY_{Lake Ontario}$	Mass exchanges between Hamilton Harbour and Lake Ontario	$F(t)$	
$YEXOG_{EPI}$	External loading	$F(t)$	
$YENDOG_x$	Internal loading	$F(t)$	
$Fe_{Steel Mills}$	Iron loading from the local steel mills	$F(t)$	kg day ⁻¹
$K_{diffusion}$	Diffusion coefficient	$F(t)$	m ² day ⁻¹
$z_{epilimnion}$	Depth of epilimnion compartment	$F(t)$	m
$z_{hypolimnion}$	Depth of hypolimnion compartment	$F(t)$	m

$F(t)$ =time-variant based on observed data from the system

Y = state variable

Table 3-ESM. Summary statistics of the exogenous flows and nutrient loadings used to reproduce the present conditions in the Hamilton Harbour.

<i>Source</i>	<i>Flow (m3/sec)</i>	<i>TP (kg/day)</i>	<i>PO4 (kg/day)</i>	<i>OP (kg/day)</i>	<i>TN (kg/day)</i>	<i>NO₃ (kg/day)</i>	<i>NH₄ (kg/day)</i>	<i>ON (kg/day)</i>
<i>Cootes Paradise</i>								
<i>Average</i>	2.569	37.8	9.5	28.3	410	111	11	288
<i>Median</i>	2.158	31.7	7.9	23.6	342	93	9	241
<i>2.50%</i>	0.817	11.9	2.9	8.9	128	35	3	89
<i>97.50%</i>	6.368	94.5	23.6	70.8	1029	278	28	727
<i>CSO</i>								
<i>Average</i>	0.297	53.9	10.7	43.1	686	412	138	136
<i>Median</i>	0.298	53.8	10.7	43.1	686	411	138	136
<i>2.50%</i>	0.235	46.4	9.0	36.2	606	345	116	114
<i>97.50%</i>	0.359	61.6	12.5	50.2	769	480	161	158
<i>Grindstone & Urban Runoff</i>								
<i>Average</i>	0.724	14.1	2.8	11.3	349	257	26	66
<i>Median</i>	0.620	12.2	2.4	9.8	299	219	22	57
<i>2.50%</i>	0.260	5.1	1.0	4.0	124	89	9	23
<i>97.50%</i>	1.693	33.1	6.6	26.4	822	605	62	156
<i>Redhill & Urban Runoff</i>								
<i>Average</i>	0.634	21.0	4.2	16.9	215	158	16	40
<i>Median</i>	0.548	18.1	3.6	14.5	185	136	14	35
<i>2.50%</i>	0.231	7.5	1.5	6.0	78	57	6	14
<i>97.50%</i>	1.443	48.3	9.5	39.2	495	366	38	94
<i>Skyway WWTP</i>								
<i>Average</i>	1.235	20.2	6.0	14.2	416	119	154	143
<i>Median</i>	1.223	20.0	5.9	14.0	412	117	152	142
<i>2.50%</i>	0.936	14.6	4.2	10.0	311	85	110	103
<i>97.50%</i>	1.596	26.9	8.2	19.2	544	160	210	193
<i>Steels Mills</i>								
<i>Average</i>		6.0	1.2	4.8	135	74	60	
<i>Median</i>		6.0	1.2	4.8	134	74	60	
<i>2.50%</i>		5.1	1.0	4.1	116	64	52	
<i>97.50%</i>		6.9	1.4	5.5	154	85	69	
<i>Woodward WWTP</i>								
<i>Average</i>	3.930	192.2	57.8	134.5	6038	2280	2997	761
<i>Median</i>	3.855	188.0	56.2	131.7	5916	2236	2926	743
<i>2.50%</i>	2.643	127.2	37.0	86.5	4019	1470	1940	488
<i>97.50%</i>	5.592	278.8	85.8	197.7	8684	3346	4428	1122
<i>Total</i>								
<i>Average</i>		344.9	92.5	252.5	8246	3410	3403	1433
<i>Median</i>		341.2	91.1	249.8	8139	3372	3333	1404
<i>2.50%</i>		259.6	68.1	189.0	6114	2534	2358	1035
<i>97.50%</i>		447.3	123.6	328.4	10970	4516	4823	1991

Table 4-ESM. Scenario 1: Summary statistics of the exogenous flows and nutrient loadings used to force the Hamilton Harbour model.

<i>Source</i>	<i>Flow (m3/sec)</i>	<i>TP (kg/day)</i>	<i>PO4 (kg/day)</i>	<i>OP (kg/day)</i>	<i>TN (kg/day)</i>	<i>NO₃ (kg/day)</i>	<i>NH₄ (kg/day)</i>	<i>ON (kg/day)</i>
<i>Cootes Paradise</i>								
<i>Average</i>	2.535	31.1	6.2	24.8	325	120	5	199
<i>Median</i>	2.100	25.5	5.1	20.5	266	99	5	163
<i>2.50%</i>	0.804	9.7	2.0	7.7	103	37	2	62
<i>97.50%</i>	6.460	80.6	16.2	64.9	833	309	14	512
<i>CSO</i>								
<i>Average</i>	0.297	25.8	5.15	20.6	627	497	67.8	62.3
<i>Median</i>	0.297	25.7	5.16	20.7	627	497	67.8	62.2
<i>2.50%</i>	0.236	22.1	4.31	17.3	543	416	56.8	52.3
<i>97.50%</i>	0.359	29.4	5.98	24	710	576	78.8	72.6
<i>Grindstone & Urban Runoff</i>								
<i>Average</i>	0.719	11.7	2.4	9.3	329	256	26	46
<i>Median</i>	0.617	10.1	2.0	8.0	282	220	22	39
<i>2.50%</i>	0.265	4.2	0.8	3.3	118	91	9	16
<i>97.50%</i>	1.690	27.1	5.5	21.7	770	602	62	109
<i>Redhill & Urban Runoff</i>								
<i>Average</i>	0.635	17.7	3.5	14.2	203	158	16	28
<i>Median</i>	0.550	15.4	3.0	12.3	175	137	14	24
<i>2.50%</i>	0.232	6.4	1.2	5.1	74	57	6	10
<i>97.50%</i>	1.439	40.4	8.1	32.5	467	366	37	65
<i>Skyway WWTP</i>								
<i>Average</i>	1.245	15.0	3.0	12.0	337	160	115	62
<i>Median</i>	1.233	14.8	2.9	11.8	334	158	113	61
<i>2.50%</i>	0.936	10.8	2.1	8.5	248	113	81	44
<i>97.50%</i>	1.612	20.1	4.1	16.3	446	219	156	85
<i>Steels Mills</i>								
<i>Average</i>		0	0	0	0	0	0	0
<i>Median</i>		0	0	0	0	0	0	0
<i>2.50%</i>		0	0	0	0	0	0	0
<i>97.50%</i>		0	0	0	0	0	0	0
<i>Woodward WWTP</i>								
<i>Average</i>	3.919	152.5	30.5	122.0	5733	3487	1790	456
<i>Median</i>	3.823	148.8	29.8	118.8	5603	3400	1750	444
<i>2.50%</i>	2.647	98.9	19.7	78.3	3788	2260	1155	294
<i>97.50%</i>	5.570	222.8	44.7	180.5	8277	5124	2655	674
<i>Total</i>								
<i>Average</i>		252.4	51.0	201.4	7646	4776	2017	853
<i>Median</i>		249.3	50.1	199.0	7521	4691	1979	833
<i>2.50%</i>		185.6	37.0	146.8	5640	3516	1385	594
<i>97.50%</i>		338.3	68.0	271.1	10200	6427	2880	1222

Table 5-ESM. Scenario 2: Summary statistics of the exogenous flows and nutrient loadings used to force the Hamilton Harbour model.

<i>Source</i>	<i>Flow (m3/sec)</i>	<i>TP (kg/day)</i>	<i>PO4 (kg/day)</i>	<i>OP (kg/day)</i>	<i>TN (kg/day)</i>	<i>NO₃ (kg/day)</i>	<i>NH₄ (kg/day)</i>	<i>ON (kg/day)</i>
<i>Cootes Paradise</i>								
<i>Average</i>	2.549	31.2	6.3	25.0	327	121	5	201
<i>Median</i>	2.122	26.0	5.3	20.7	273	102	5	167
<i>2.50%</i>	0.796	9.8	1.9	7.7	102	37	2	62
<i>97.50%</i>	6.423	79.4	16.1	63.0	831	307	14	507
<i>CSO</i>								
<i>Average</i>	0.298	25.8	5.2	20.6	627	497	68	62
<i>Median</i>	0.299	25.7	5.2	20.7	627	497	68	62
<i>2.50%</i>	0.235	22.2	4.3	17.3	543	417	57	52
<i>97.50%</i>	0.360	29.4	6.0	24.0	710	577	79	73
<i>Grindstone & Urban Runoff</i>								
<i>Average</i>	0.734	12.0	2.4	9.5	335	261	27	47
<i>Median</i>	0.640	10.4	2.1	8.3	293	227	23	41
<i>2.50%</i>	0.265	4.2	0.8	3.4	119	91	9	17
<i>97.50%</i>	1.721	27.7	5.7	22.2	778	609	62	109
<i>Redhill & Urban Runoff</i>								
<i>Average</i>	0.642	17.9	3.6	14.3	205	160	16	29
<i>Median</i>	0.561	15.7	3.1	12.5	179	139	14	25
<i>2.50%</i>	0.235	6.4	1.3	5.1	74	57	6	10
<i>97.50%</i>	1.453	40.4	8.0	32.8	465	364	37	65
<i>Skyway WWTP</i>								
<i>Average</i>	1.240	14.9	3.0	12.0	336	159	115	62
<i>Median</i>	1.227	14.7	2.9	11.8	331	157	113	61
<i>2.50%</i>	0.937	10.8	2.1	8.5	246	113	81	44
<i>97.50%</i>	1.609	20.1	4.0	16.3	444	218	157	84
<i>Steels Mills</i>								
<i>Average</i>		0	0	0	0	0	0	0
<i>Median</i>		0	0	0	0	0	0	0
<i>2.50%</i>		0	0	0	0	0	0	0
<i>97.50%</i>		0	0	0	0	0	0	0
<i>Woodward WWTP</i>								
<i>Average</i>	3.910	118.6	23.6	95.0	5480	4359	893	228
<i>Median</i>	3.833	115.5	23.1	92.3	5355	4251	873	222
<i>2.50%</i>	2.627	77.1	15.1	60.6	3617	2824	580	147
<i>97.50%</i>	5.545	173.7	34.5	140.5	7900	6401	1326	337
<i>Total</i>								
<i>Average</i>		219.2	44.2	175.1	7396	5632	1128	637
<i>Median</i>		216.5	43.6	173.1	7252	5508	1104	610
<i>2.50%</i>		160.6	32.3	127.3	5458	4091	812	431
<i>97.50%</i>		294.7	59.3	237.0	9833	7616	1567	977

Table 6-ESM. Summary statistics of the exogenous flows and nutrient loadings reflecting the Hamilton Harbour RAP recommendations.

<i>Source</i>	<i>Flow (m3/sec)</i>	<i>TP (kg/day)</i>	<i>PO4 (kg/day)</i>	<i>OP (kg/day)</i>	<i>TN (kg/day)</i>	<i>NO₃ (kg/day)</i>	<i>NH₄ (kg/day)</i>	<i>ON (kg/day)</i>
<i>Cootes Paradise</i>								
<i>Average</i>	2.587	31.7	6.4	25.4	332	123	6	204
<i>Median</i>	2.157	26.4	5.3	21.0	275	102	5	168
<i>2.50%</i>	0.805	9.8	2.0	7.8	102	37	2	62
<i>97.50%</i>	6.448	79.1	15.8	63.6	835	310	14	512
<i>CSO</i>								
<i>Average</i>	0.297	4.9	1.0	4.0	573	543	21	8
<i>Median</i>	0.297	4.9	1.0	4.0	573	543	21	8
<i>2.50%</i>	0.235	4.2	0.8	3.3	485	455	18	7
<i>97.50%</i>	0.359	5.6	1.1	4.6	660	630	25	10
<i>Grindstone & Urban Runoff</i>								
<i>Average</i>	0.716	11.6	2.3	9.3	327	255	26	46
<i>Median</i>	0.619	10.1	2.0	8.1	282	220	23	40
<i>2.50%</i>	0.263	4.2	0.8	3.3	118	92	9	16
<i>97.50%</i>	1.633	26.3	5.4	21.0	742	582	60	105
<i>Redhill & Urban Runoff</i>								
<i>Average</i>	0.628	17.5	3.5	14.0	200	156	16	28
<i>Median</i>	0.536	15.0	3.0	12.0	171	133	14	24
<i>2.50%</i>	0.232	6.4	1.3	5.1	73	57	6	10
<i>97.50%</i>	1.436	40.2	8.1	32.4	462	362	37	65
<i>Skyway WWTP</i>								
<i>Average</i>	1.242	11.9	2.4	9.5	336	160	115	62
<i>Median</i>	1.226	11.8	2.3	9.5	332	157	114	61
<i>2.50%</i>	0.937	8.6	1.7	6.8	250	115	82	44
<i>97.50%</i>	1.609	16.0	3.2	13.0	447	218	158	84
<i>Steels Mills</i>								
<i>Average</i>		0	0	0	0	0	0	0
<i>Median</i>		0	0	0	0	0	0	0
<i>2.50%</i>		0	0	0	0	0	0	0
<i>97.50%</i>		0	0	0	0	0	0	0
<i>Woodward WWTP</i>								
<i>Average</i>	3.943	59.3	12.2	47.1	5421	4774	540	107
<i>Median</i>	3.867	58.3	11.9	46.3	5305	4669	528	105
<i>2.50%</i>	2.674	38.7	7.9	30.3	3542	3079	349	69
<i>97.50%</i>	5.547	86.0	17.8	69.4	7893	7009	796	157
<i>Total</i>								
<i>Average</i>		136.5	27.9	108.6	7268	6075	727	466
<i>Median</i>		133.2	27.3	106.1	7158	5978	716	434
<i>2.50%</i>		93.3	19.0	73.9	5295	4362	527	288
<i>97.50%</i>		196.9	40.1	157.4	9781	8289	984	795